$Kit^-CD203c^-HLA\text{-}DR^-$ cells from BM of hSCF Tg and non-Tg NSG recipients. In 9 of 13 hSCF Tg recipient BM cells examined, the majority of myeloid cells showed the morphology of immature granulocytes with large nuclear-to-cytoplasmic ratio and nuclei with few lobulations, largely consisting of myelocytes and metamyelocytes (S4-1 and S12-2 shown as representative in Figure 2E). In 4 of 13 hSCF Tg recipients examined and in 4 of 5 non-Tg NSG recipients, mature segmented neutrophils were present in the sorted $CD33^+c\text{-}Kit^-CD203c^-HLA\text{-}DR^-$ granulocyte population (N12-1 and S2-1 shown as representative in Figure 2E). These findings indicate that both by quantitative and morphologic examinations, human granulocytic cells with various degrees of maturity predominate among the $CD33^+$ myeloid cells developing within the hSCF Tg NSG recipients. To examine the myeloid differentiation capacity of hematopoietic stem and progenitor populations in a functional manner, we performed a colony-forming cell assay using $CD34^+CD38^-$ and $CD34^+CD38^+$ cells derived from BM of hSCF Tg NSG recipients and non-Tg NSG recipients. In both cell populations, myeloid and erythroid colony formation were similar between hSCF Tg NSG and non-Tg NSG recipient BM (supplemental Figure 3).

We then analyzed global transcriptional profiles of $CD33^+HLA\text{-}DR^-c\text{-}Kit^-CD203c^-$ granulocytes from hSCF Tg NSG recipient BM (n = 4), non-Tg NSG recipient BM (n = 3), and primary human BM (n = 2). Additional control samples included BM monocytes from hSCF Tg recipients (n = 3), non-Tg NSG recipient BM monocytes (n = 3), and primary human BM monocytes (n = 2). Unsupervised clustering demonstrated a clear segregation of transcriptional profiles between granulocytes and monocytes regardless of the source. This suggests that human granulocytes and monocytes in humanized mouse undergo a distinct differentiation process similar to their counterparts in human BM (Figure 2F). We next examined whether there were any differences in gene expression within 3 distinct granulocyte sources (hSCF Tg recipient BM, non-Tg NSG recipient BM, and primary human BM neutrophils; Figure 2G). As seen in the heatmap representation, we found clusters of genes differentially transcribed in the distinct sources of granulocytes (Figure 2G). Multiple genes associated with transcriptional regulation were included in the genes upregulated in human immature granulocytes derived from the BM of hSCF Tg NSG mice, suggesting that these cells are more actively cycling and proliferating compared with mature granulocytes from the BM of hSCF Tg NSG and non-Tg NSG mice and primary human BM neutrophils (Figure 2G; supplemental Tables 1 and 2).

Development of human mast cells in hSCF Tg NSG recipients

We next investigated the development of human mast cells in the membrane-bound hSCF-expressing NSG mice. Overall, the frequencies of $cKit^+CD203c^+$ cells within total BM $CD33^+$ myeloid cells were similar between hSCF Tg NSG and non-Tg NSG recipients when excluding 2 non-Tg NSG recipients observed for more than 8 months ($P = .1439$ by 2-tailed t test; Figure 2D; Table 1). In 7 of 20 hSCF Tg NSG recipients, compared with one of 10 non-Tg NSG recipients, the frequency of $cKit^+CD203c^+$ cells in BM $CD33^+$ cells was greater than 15% (Figure 2D; Table 1). When these $cKit^+CD203c^+$ cells were FACS-purified and examined by MGG staining, their morphology was consistent with mast cells with various degrees of cytoplasmic granulation (Figure 3A-B). Histologic examination of H&E-stained bone sections showed increased cellularity in hSCF Tg NSG recipients compared with non-Tg NSG recipients (Figure 3C). We then performed IHC staining for mast cell tryptase to identify human mast cells in the BM. Consistent with the quantitative analysis by flow cytometry, $tryptase^+$ cells were abundantly observed in the hSCF Tg NSG recipients compared with non-Tg NSG recipients (Figure 3C). This does not reflect an increase in mouse mast cells because nearly all nucleated hematopoietic cells in the hSCF Tg NSG recipients are of human origin (Figure 1D). The same sections were further subjected to the immunofluorescence staining followed by confocal imaging demonstrating that these are mast cells and not $CD14^+$ monocytes (supplemental Figure 4).

Mast cell progenitors and mature mast cells reside in high frequencies in the spleen of normal immunocompetent mice.[21] We next examined the spleen of human HSC-engrafted hSCF Tg NSG recipients. Human $CD33^{high}c\text{-}Kit^+CD203c^+$ mast cells accounted for the highest frequency among total $hCD45^+hCD33^+$ myeloid cells in the spleen of both hSCF Tg NSG and non-Tg NSG HSC-engrafted recipients (Figure 4A-B). However, the frequencies of human mast cells in the myeloid cell population were significantly higher in hSCF Tg NSG recipients than in non-Tg NSG controls (hSCF Tg: 77.4% ± 4.5%; n = 20 and non-Tg NSG controls: 62.5% ± 3.9%; n = 12; $P = .0304$ by 2-tailed t test; Figure 4B). These human cells with surface expression phenotype of mast cells also showed morphologic features of mature mast cells (Figure 4C). Mast cell tryptase IHC staining confirmed the presence of human mast cells within the recipient spleen (Figure 4D). These findings indicate that the expression of membrane-bound human SCF in the recipient mouse microenvironment enhances development of human mast cells from transplanted human HSCs within hematopoietic organs, such as the BM and spleen, consistent with the activation of c-Kit signaling.

Next, we investigated whether the transgenic expression of hSCF results in the efficient development of mucosal tissue-type human mast cells in respiratory and gastrointestinal mucosal layers, as well as in hematopoietic organs. For this purpose, we performed IHC staining of human tryptase-expressing mast cells in the lung, stomach, small intestine, and large intestine in hSCF Tg NSG and non-Tg NSG recipients. In the hSCF Tg NSG recipient lungs, human tryptase-positive mast cells were identified within cellular infiltrates (supplemental Figure 5). In tissue sections from the stomach, small intestine, and large intestine, human tryptase-positive mast cells were present in both hSCF Tg NSG and non-Tg NSG recipients (Figure 5A-B). The mast cell $tryptase^+$ cells in gastrointestinal tissues of hSCF Tg mice were further examined by immunofluorescence microscopy using anti–human CD45 and anti–human-c-Kit antibodies. We found the presence of $hCD45^+c\text{-}Kit^+$ cells in the gastric tissues of the hSCF Tg recipients consistent with IHC staining for mast cell tryptase (Figure 5C). Because gastric tissue is one of the major sites of mast cell populations in humans and mice, we quantified human mast cells in the gastric tissue of hSCF Tg and non-Tg NSG recipients transplanted with human HSCs. IHC staining for human mast cell tryptase followed by quantification of $tryptase^+$ cells demonstrated the presence of human mast cells in gastric tissues of hSCF Tg NSG recipients (7.01% ± 0.63%, 3 sites per recipient analyzed in 3 mice) compared with non-Tg NSG recipients (2.53% ± 0.53%, 3 sites per recipient analyzed in 3 mice; $P < .0001$ by 2-tailed t test; Figure 5D). Collectively, transgenic expression of human membrane-bound SCF influences human myeloid development and mast cell development in hematopoietic organs and mucosal tissues along with the achievement of high chimerism of human hematopoietic cells in hematopoietic organs.

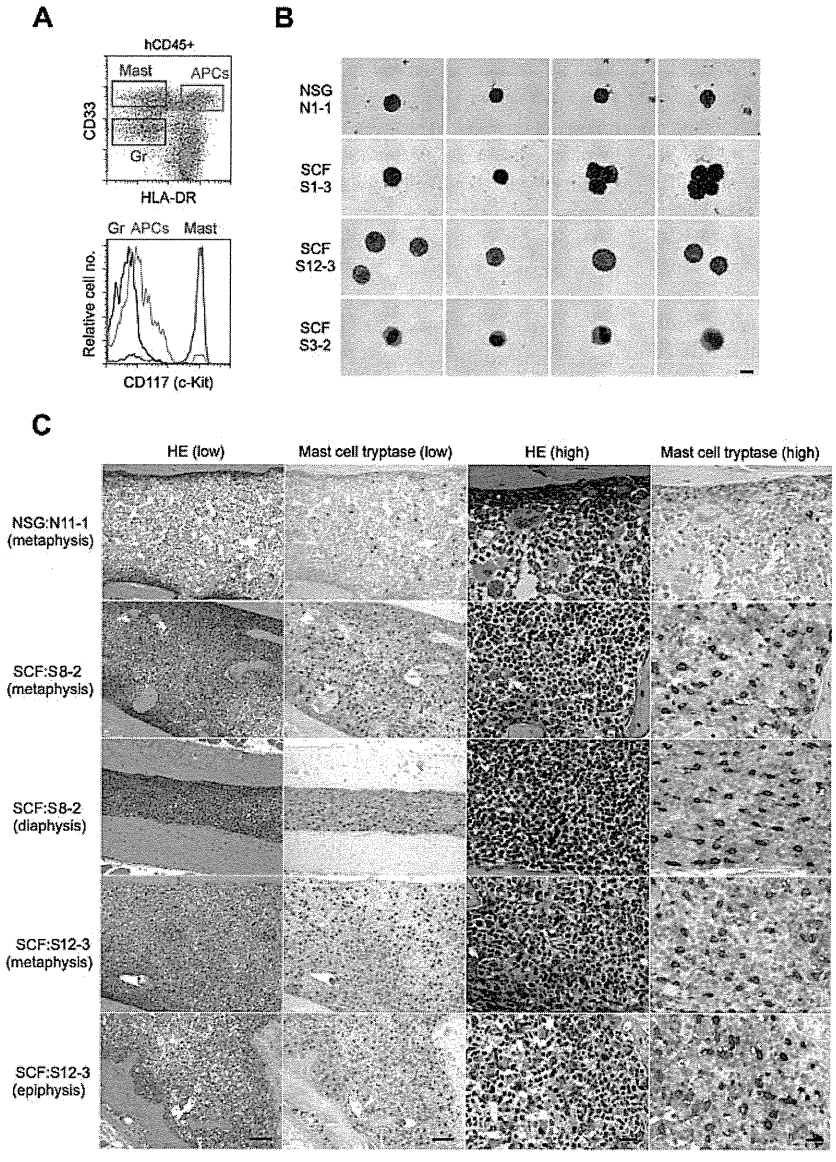

Figure 3. Human mast cell development in hSCF Tg NSG recipient BM. (A) Representative flow cytometric scatter plot and histogram demonstrating the identification of human $CD45^+CD33^+CD117^+$ mast cells. (B) FACS-sorted $hCD45^+CD33^+CD117^+CD203c^+$ human mast cells from a representative non-Tg NSG recipient BM (N1-1, 0.9% human mast cells within $hCD45^+CD33^+$ population) and hSCF Tg NSG recipient BM (S1-3, 14.6%; S12-3, 8.8%; and S3-2, 7.3% human mast cells within the $hCD45^+CD33^+$ population) were examined by MGG staining (N1-1, killed at 21 weeks; S1-3, killed at 21 weeks; S12-3, killed at 13 weeks; and S3-2, killed at 15 weeks). (C) H&E- and anti-mast cell tryptase antibody–stained bone sections demonstrate hypercellular BM with high frequency of $tryptase^+$ human mast cells in hSCF Tg NSG recipients. Non-Tg NSG recipient: N11-1, 70.7% $hCD45^+$. hSCF Tg NSG recipients: S8-2, 99.6%; and S12-3, 79.5% $hCD45^+$ (N11-1, killed at 20 weeks; S8-2, killed at 11 weeks; and S12-3, killed at 13 weeks).

Discussion

A supportive microenvironment is essential for hematopoietic and immune system homeostasis. Critical roles played by various niches in the maintenance of cell cycle quiescence and self-renewal capacity of HSCs have been demonstrated, and the thymic microenvironment is critical for T-cell education.[22,23] However, despite significant progress over the last decade, the stromal microenvironment within the humanized mouse is predominately of mouse origin. Although several key molecules, such as SDF1, are cross-reactive between human and mouse, a humanized microenvironment is required both to further improve human hematopoietic development in the recipients and to investigate in vivo the interactions between hematopoietic cells and their microenvironment.

In the present study, we humanized membrane-bound stem cell factor [SCF = KIT ligand (KL)] using the construct and mouse strain created by Majumdar et al.[13] Toksoz et al reported that human membrane-bound SCF expressed by mouse stromal cells efficiently supports long-term human hematopoiesis in vitro.[24] The importance of SCF interaction with $cKit^+$ HSCs and mast cell progenitors in murine hematopoiesis is highlighted by the hematopoietic abnormalities in mice with *Kitl* and *Kit* mutations.[25-27] In human hematopoiesis, SCF-cKit signaling is critical for the maintenance of stem and progenitor cell activities.[28] Human SCF/KL has been shown to drive cell-cycle entry by primitive hematopoietic cells in vitro.[29] Both long-term colony-initiation and colony-forming capacities are expanded ex vivo by cytokine supplementation that includes SCF/KL.[30-32] Therefore, to elucidate the role of membrane-bound human SCF in differentiation, proliferation, and maturation of human hematopoiesis in vivo, we created a novel NSG mouse strain that can support the engraftment of human HSCs and express hSCF in microenvironment. In hSCF Tg NSG recipients transplanted with human HSCs, the engraftment levels of human $CD45^+$ cells were significantly higher compared with non-Tg NSG controls. Majumdar et al reported that human SCF binds mouse c-Kit receptor but that the binding affinity is

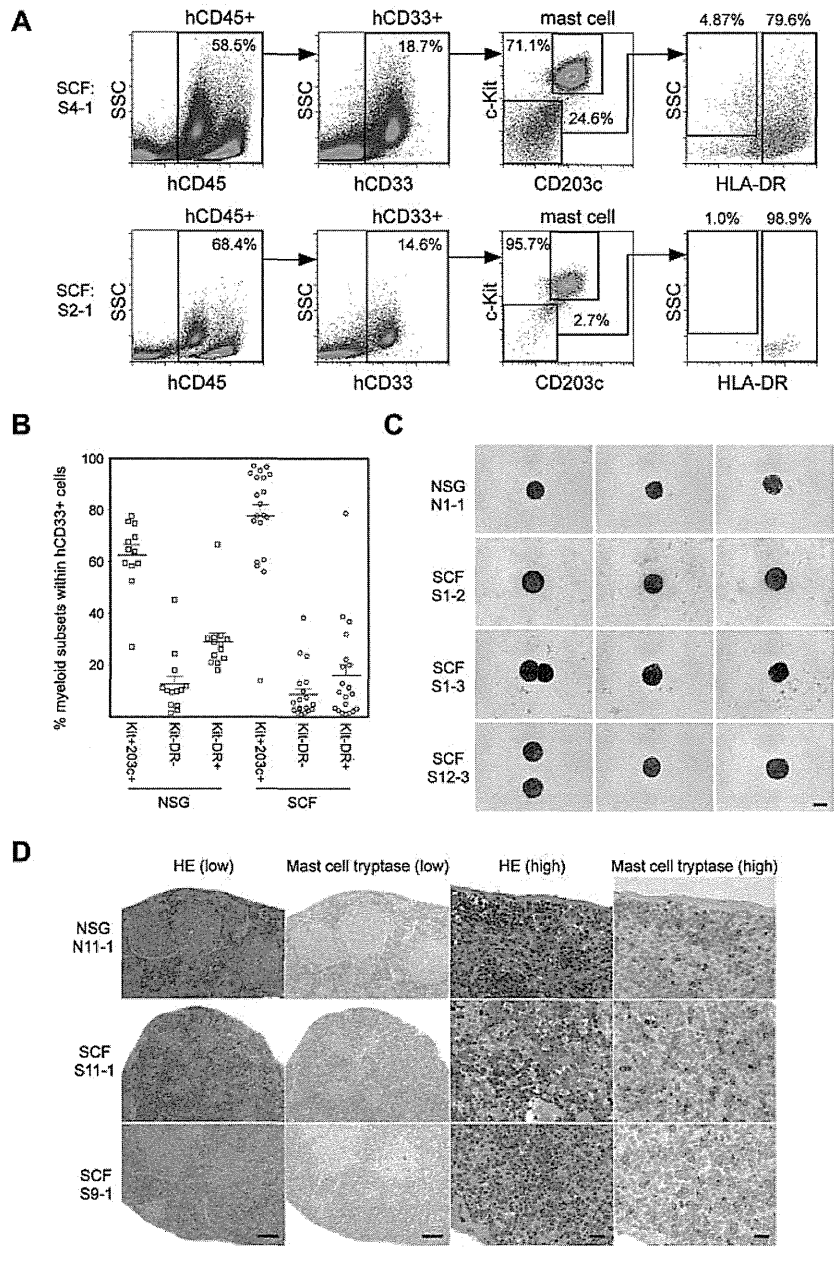

Figure 4. Human mast cell development in hSCF Tg NSG recipient spleen. (A) Human mast cell development is enhanced in hSCF Tg NSG recipient spleens (S4-1, killed at 13 weeks; and S2-1, killed at 16 weeks). (B) Frequencies of human c-Kit$^+$CD203c$^+$ mast cells, CD33$^+$HLA-DR$^-$ granulocyte population, and CD33$^+$HLA-DR$^+$ APCs within total hCD45$^+$hCD33$^+$ myeloid cells in the spleens of hSCF Tg and non-Tg NSG recipients. Human mast cell development in the spleen was significantly greater in the hSCF Tg NSG recipients (hSCF Tg: n = 20, non-Tg NSG: n = 12, $P = .0304$). (C) FACS-sorted hCD45$^+$CD33$^+$CD117$^+$CD203c$^+$ human mast cells from a representative non-Tg NSG recipient spleen (N1-1, 59.3% human mast cells within hCD45$^+$CD33$^+$ population) and hSCF Tg NSG recipient spleen (S1-2, 85.7%; S1-3, 77.7%; and S12-3, 56.1% human mast cells within hCD45$^+$CD33$^+$ population) were examined by MGG staining (N1-1, killed at 21 weeks; S1-2, killed at 20 weeks; S1-3, killed at 21 weeks; and S12-3, killed at 13 weeks). (D) H&E- and anti–mast cell tryptase antibody–stained spleen sections demonstrating the presence of human mast cells in non-Tg NSG recipients and hSCF Tg NSG recipients (non-Tg NSG recipient: N11-1, 94.0% hCD45$^+$; hSCF Tg NSG recipients: S11-1, 95.3%; and S9-1, 97.0% hCD45$^+$; N11-1, killed at 20 weeks; S11-1, killed at 10 weeks; and S9-1, killed at 16 weeks).

weaker compared with the binding affinity of human SCF to human c-Kit.[13] Therefore, the significant improvement of human hematopoietic chimerism could be attributed to preferential binding of human SCF to human HSCs instead of murine c-Kit$^+$ HSCs resulting in accelerated signaling through c-Kit in human HSCs and by impaired or attenuated support of mouse HSCs.[1,33,34] Presumably because of the competition between human and mouse hematopoietic stem or myeloid/erythroid progenitor cells, we observed diminished mouse erythrocyte hemoglobin concentration with normal range of mean corpuscular volume, mean corpuscular hemoglobin, and mean corpuscular hemoglobin concentration in all the 21 hSCF Tg NSG recipients but not in any of the non-Tg NSG recipients or nontransplanted hSCF Tg NSG adults. In addition to the greatly increased levels of human hematopoietic repopulation, we identified significant differences in human hematopoietic differentiation in hSCF Tg NSG recipients compared with non-Tg NSG recipients. Namely, there were substantially increased levels of human myeloid differentiation from HSCs in the hSCF Tg NSG mice, whereas human B cells accounted for the greatest population in the BM of non-Tg NSG mice. Because normal human BM contains myeloid cells at a relatively high frequency (36.2%-62.2%),[35] human SCF may be important in recapitulating human BM myelopoiesis in immunodeficient mice. In addition, membrane-bound human SCF may exert distinct effects on human myeloid development in the BM and in the spleen. In the BM of hSCF Tg recipients, the majority of human myeloid cells were c-Kit$^-$CD203c$^-$HLA-DR$^-$ granulocytes. Among these granulocytes, myeloid cells at various levels of maturity were identified, with myelocytes and metamyelocytes predominating in the majority of hSCF Tg NSG recipients. Because immature cells were more prominent in hSCF Tg NSG recipients compared with non-Tg NSG recipients, we performed microarray analysis to

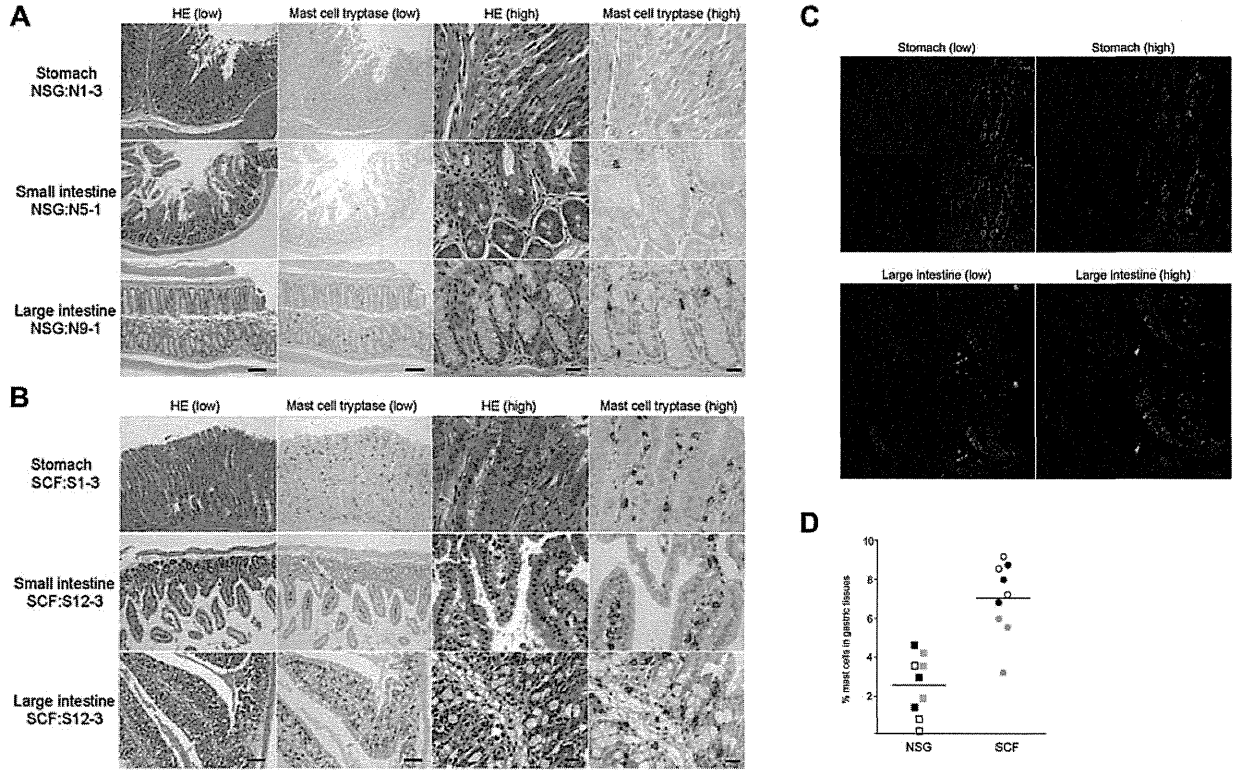

Figure 5. Human mast cell development in hSCF Tg NSG recipient stomach, small intestine, and large intestine. H&E- and anti–mast cell tryptase antibody–stained sections of (A) non-Tg NSG recipient stomach (NSG control, N1-3), small intestine (N5-1), and large intestine (N9-1) and (B) hSCF Tg NSG recipient stomach (S1-3), small intestine (S12-3), and large intestine (S12-3) demonstrating the presence of human mast cells (N1-3, killed at 24 weeks; N5-1, killed at 35 weeks; N9-1, killed at 20 weeks; S1-3, killed at 21 weeks; and S12-3, killed at 13 weeks). (C) Confocal immunofluorescence images of hSCF Tg stomach (S1-9) demonstrate human CD45$^+$ (green) and human CD117$^+$ (red) mast cells. (D) Frequencies of tryptase$^+$ cells were quantified by sampling 3 areas each from hSCF Tg (n = 3) and non-Tg (n = 3) NSG recipients: hSCF Tg NSG recipients, 7.0% ± 0.6%; and non-Tg NSG recipients, 2.5% ± 0.5% ($P < .0001$ by 2-tailed t test).

identify transcriptional signature specific to the immature human granulocytes that developed in the hSCF Tg NSG mice. Approximately 300 genes were differentially transcribed in the immature granulocytes in hSCF Tg NSG recipients compared with the mature granulocytes in non-Tg NSG recipients. Some of the up-regulated genes were associated with cell cycle or metabolism.

In several hSCF Tg NSG recipients, human mast cells composed the greatest subfraction among engrafted human myeloid cells. In the spleens of hSCF Tg NSG-engrafted mice, human mast cells were present at the highest frequency among the myeloid lineage developed in the recipients. MGG staining revealed both mature and immature mast cells in hSCF Tg NSG recipient BM. Human mast cells were identified not only in hematopoietic organs but also in lung, gastric tissue, and intestinal tissues of hSCF Tg NSG recipients. Aberrant expression of CD30 and CD25 on mast cells is associated with systemic mastocytosis and other mast cell disorders.[36,37] We did not find significantly up-regulated expression of these antigens in the mast cells derived from BM or spleen of hSCF Tg NSG recipients.

To date, several mouse strains have been developed for supporting normal and malignant human hematopoietic cell engraftment and normal myeloid cell differentiation using *Il2rg*^{null} immune-compromised mice (supplemental Table 3).[5,6,8,9,20,38-41] Among these, human thrombopoietin knock-in *Rag2*^{null} *Il2rg*^{null} mice were reported to support both human hematopoietic engraftment and myeloid differentiation in the BM. Both SCF and thrombopoietin exhibit species specificity between humans and mouse in supporting HSCs and myeloid cells in both species. These approaches focusing on the 2 distinct molecules based on the 2 immune-compromised mouse backgrounds will allow us to investigate human hematopoiesis and immunity from stem cells to myeloid progenitors to mature myeloid effecter cells in vivo. Altogether, the newly created hSCF Tg NSG mouse model engrafted with purified human HSCs will facilitate the in vivo understanding of human hematopoietic hierarchy and mast cell biology.

Acknowledgments

The authors thank David Williams for providing C3H/HeJ mice carrying the human SCF transgene and Dr Kodo and his staff at the Tokyo Cord Blood Bank for their generous assistance in processing and providing cord blood samples.

This work was supported by the National Institutes of Health (research grants HL077642, CA34196, AI46629, UO1 AI073871, DK089572), the University of Massachusetts Center for AIDS Research (P30 AI042845), the Juvenile Diabetes Foundation, International, the Helmsley Foundation, USAMRIID (L.D.S.), Project for Developing Innovation Systems, Program for Fostering Regional Innovation (O.O.), Takeda Science Foundation and Ministry of Education, Culture, Sports, Science and Technology, Japan (F.I.), and the Japan Society for the Promotion of Science through the Funding Program for Next Generation World-Leading Researchers (NEXT Program), initiated by the Council for Science and Technology Policy.

The contents of this publication are solely the responsibility of the authors and do not necessarily represent the official views of the National Institutes of Health.

Authorship

Contribution: S. Takagi, S. Tanaka, T.H., and S.M. performed the experiments; A.H., T.W., and O.O. performed and analyzed the microarray experiments; J.K., H. Kiyono, H. Koseki, O.O., T.S., and S. Taniguchi participated in discussions on research planning and analysis of results; and S. Takagi, Y.S., L.D.S., and F.I. designed the research and wrote the paper.

Conflict-of-interest disclosure: The authors declare no competing financial interests.

Correspondence: Fumihiko Ishikawa, Research Unit for Human Disease Models, RIKEN Research Center for Allergy and Immunology, 1-7-22 Suehiro-cho Tsurumi-ku, Yokohama, Kanagawa, Japan 230-0045; e-mail: f_ishika@rcai.riken.jp.

References

1. Manz MG. Human-hemato-lymphoid-system mice: opportunities and challenges. *Immunity.* 2007;26(5):537-541.
2. Shultz LD, Ishikawa F, Greiner DL. Humanized mice in translational biomedical research. *Nat Rev Immunol.* 2007;7(2):118-130.
3. McCune JM, Namikawa R, Kaneshima H, Shultz LD, Lieberman M, Weissman IL. The SCID-hu mouse: murine model for the analysis of human hematolymphoid differentiation and function. *Science.* 1988;241(4873):1632-1639.
4. Mosier DE, Gulizia RJ, Baird SM, Wilson DB. Transfer of a functional human immune system to mice with severe combined immunodeficiency. *Nature.* 1988;335(6187):256-259.
5. Ishikawa F, Yasukawa M, Lyons B, et al. Development of functional human blood and immune systems in NOD/SCID/IL2 receptor gamma chain-(null) mice. *Blood.* 2005;106(5):1565-1573.
6. Ito M, Hiramatsu H, Kobayashi K, et al. NOD/SCID/gamma(c)(null) mouse: an excellent recipient mouse model for engraftment of human cells. *Blood.* 2002;100(9):3175-3182.
7. Shultz LD, Banuelos S, Lyons B, et al. NOD/LtSz-Rag1nullPfpnull mice: a new model system with increased levels of human peripheral leukocyte and hematopoietic stem-cell engraftment. *Transplantation.* 2003;76(7):1036-1042.
8. Shultz LD, Lyons BL, Burzenski LM, et al. Human lymphoid and myeloid cell development in NOD/LtSz-scid IL2R gamma null mice engrafted with mobilized human hemopoietic stem cells. *J Immunol.* 2005;174(10):6477-6489.
9. Traggiai E, Chicha L, Mazzucchelli L, et al. Development of a human adaptive immune system in cord blood cell-transplanted mice. *Science.* 2004; 304(5667):104-107.
10. Strowig T, Gurer C, Ploss A, et al. Priming of protective T cell responses against virus-induced tumors in mice with human immune system components. *J Exp Med.* 2009;206(6):1423-1434.
11. Jaiswal S, Pearson T, Friberg H, et al. Dengue virus infection and virus-specific HLA-A2 restricted immune responses in humanized NOD-scid IL2rgammanull mice. *PLoS One.* 2009;4(10): e7251.
12. Shultz LD, Saito Y, Najima Y, et al. Generation of functional human T-cell subsets with HLA-restricted immune responses in HLA class I expressing NOD/SCID/IL2r gamma(null) humanized mice. *Proc Natl Acad Sci U S A.* 2010; 107(29):13022-13027.
13. Majumdar MK, Everett ET, Xiao X, et al. Xenogeneic expression of human stem cell factor in transgenic mice mimics codominant c-kit mutations. *Blood.* 1996;87(8):3203-3211.
14. Hong F, Breitling R, McEntee CW, et al. RankProd: a bioconductor package for detecting differentially expressed genes in meta-analysis. *Bioinformatics.* 2006;22(22):2825-2827.
15. Draghici S, Khatri P, Martins RP, et al. Global functional profiling of gene expression. *Genomics.* 2003;81(2):98-104.
16. Benjamini Y, Hochberg Y, et al. Controlling the false discovery rate: a practical and powerful approach to multiple testing. *J R Stat Soc B Met.* 1995;57(1):289-300.
17. Kawashima I, Zanjani ED, Almaida-Porada G, Flake AW, Zeng H, Ogawa M. CD34+ human marrow cells that express low levels of Kit protein are enriched for long-term marrow-engrafting cells. *Blood.* 1996;87(10):4136-4142.
18. Sakabe H, Kimura T, Zeng Z, et al. Haematopoietic action of flt3 ligand on cord blood-derived CD34-positive cells expressing different levels of flt3 or c-kit tyrosine kinase receptor: comparison with stem cell factor. *Eur J Haematol.* 1998;60(5): 297-306.
19. Yoshikubo T, Inoue T, Noguchi M, Okabe H. Differentiation and maintenance of mast cells from CD34+ human cord blood cells. *Exp Hematol.* 2006;34(3):320-329.
20. Hiramatsu H, Nishikomori R, Heike T, et al. Complete reconstitution of human lymphocytes from cord blood CD34+ cells using the NOD/SCID/gammacnull mice model. *Blood.* 2003;102(3): 873-880.
21. Arinobu Y, Iwasaki H, Gurish MF, et al. Developmental checkpoints of the basophil/mast cell lineages in adult murine hematopoiesis. *Proc Natl Acad Sci U S A.* 2005;102(50):18105-18110.
22. Kiel MJ, Morrison SJ. Uncertainty in the niches that maintain haematopoietic stem cells. *Nat Rev Immunol.* 2008;8(4):290-301.
23. Jenkinson EJ, Jenkinson WE, Rossi SW, Anderson G. The thymus and T-cell commitment: the right niche for Notch? *Nat Rev Immunol.* 2006;6(7):551-555.
24. Toksoz D, Zsebo KM, Smith KA, et al. Support of human hematopoiesis in long-term bone marrow cultures by murine stromal cells selectively expressing the membrane-bound and secreted forms of the human homolog of the steel gene product, stem cell factor. *Proc Natl Acad Sci U S A.* 1992;89(16):7350-7354.
25. Besmer P, Manova K, Duttlinger R, et al. The kit-ligand (steel factor) and its receptor c-kit/W: pleiotropic roles in gametogenesis and melanogenesis. *Dev Suppl.* 1993;125-137.
26. Geissler EN, McFarland EC, Russell ES. Analysis of pleiotropism at the dominant white-spotting (W) locus of the house mouse: a description of ten new W alleles. *Genetics.* 1981;97(2):337-361.
27. Russell ES. Hereditary anemias of the mouse: a review for geneticists. *Adv Genet.* 1979;20:357-459.
28. Broudy VC. Stem cell factor and hematopoiesis. *Blood.* 1997;90(4):1345-1364.
29. Leary AG, Zeng HQ, Clark SC, Ogawa M. Growth factor requirements for survival in G0 and entry into the cell cycle of primitive human hemopoietic progenitors. *Proc Natl Acad Sci U S A.* 1992; 89(9):4013-4017.
30. Bernstein ID, Andrews RG, Zsebo KM. Recombinant human stem cell factor enhances the formation of colonies by CD34+ and CD34+lin− cells, and the generation of colony-forming cell progeny from CD34+lin− cells cultured with interleukin-3, granulocyte colony-stimulating factor, or granulocyte-macrophage colony-stimulating factor. *Blood.* 1991;77(11):2316-2321.
31. Haylock DN, To LB, Dowse TL, Juttner CA, Simmons PJ. Ex vivo expansion and maturation of peripheral blood CD34+ cells into the myeloid lineage. *Blood.* 1992;80(6):1405-1412.
32. Petzer AL, Hogge DE, Landsdorp PM, Reid DS, Eaves CJ. Self-renewal of primitive human hematopoietic cells (long-term-culture-initiating cells) in vitro and their expansion in defined medium. *Proc Natl Acad Sci U S A.* 1996;93(4):1470-1474.
33. Lev S, Yarden Y, Givol D. Dimerization and activation of the kit receptor by monovalent and bivalent binding of the stem cell factor. *J Biol Chem.* 1992;267(22):15970-15977.
34. Martin FH, Suggs SV, Langley KE, et al. Primary structure and functional expression of rat and human stem cell factor DNAs. *Cell.* 1990;63(1):203-211.
35. Terstappen LW, Safford M, Loken MR. Flow cytometric analysis of human bone marrow: III. Neutrophil maturation. *Leukemia.* 1990;4(9):657-663.
36. Pardanani A. Systemic mastocytosis in adults: 2011 update on diagnosis, risk stratification, and management. *Am J Hematol.* 2011;86(4):362-371.
37. Sotlar K, Cerny-Reiterer S, Petat-Dutter K, et al. Aberrant expression of CD30 in neoplastic mast cells in high-grade mastocytosis. *Mod Pathol.* 2011;24(4):585-595.
38. Rongvaux A, Willinger T, Takizawa H, et al. Human thrombopoietin knockin mice efficiently support human hematopoiesis in vivo. *Proc Natl Acad Sci U S A.* 2011;108(6):2378-2383.
39. Pearson T, Shultz LD, Miller D, et al. Non-obese diabetic-recombination activating gene-1 (NOD-Rag1 null) interleukin (IL)-2 receptor common gamma chain (IL2r gamma null) null mice: a radioresistant model for human lymphohaematopoietic engraftment. *Clin Exp Immunol.* 2008;154(2): 270-284.
40. Brehm MA, Cuthbert A, Yang C, et al. Parameters for establishing humanized mouse models to study human immunity: analysis of human hematopoietic stem cell engraftment in three immunodeficient strains of mice bearing the IL2rgamma(null) mutation. *Clin Immunol.* 2010;135(1):84-98.
41. Strowig T, Rongvaux A, Rathinam C, et al. Transgenic expression of human signal regulatory protein alpha in Rag2−/−gammac−/− mice improves engraftment of human hematopoietic cells in humanized mice. *Proc Natl Acad Sci U S A.* 2011;108(32):13218-13223.

Published May 18, 2012, doi:10.4049/jimmunol.1103660

Development of Mature and Functional Human Myeloid Subsets in Hematopoietic Stem Cell-Engrafted NOD/SCID/IL2rγKO Mice

Satoshi Tanaka,*,†,‡,§ Yoriko Saito,‡ Jun Kunisawa,*,† Yosuke Kurashima,† Taichi Wake,† Nahoko Suzuki,‡ Leonard D. Shultz,¶ Hiroshi Kiyono,*,†,‖ and Fumihiko Ishikawa‡

Although physiological development of human lymphoid subsets has become well documented in humanized mice, in vivo development of human myeloid subsets in a xenotransplantation setting has remained unevaluated. Therefore, we investigated in vivo differentiation and function of human myeloid subsets in NOD/SCID/IL2rγ^{null} (NSG) mouse recipients transplanted with purified lineage$^-$CD34$^+$CD38$^-$ cord blood hematopoietic stem cells. At 4–6 mo posttransplantation, we identified the development of human neutrophils, basophils, mast cells, monocytes, and conventional and plasmacytoid dendritic cells in the recipient hematopoietic organs. The tissue distribution and morphology of these human myeloid cells were similar to those identified in humans. After cytokine stimulation in vitro, phosphorylation of STAT molecules was observed in neutrophils and monocytes. In vivo administration of human G-CSF resulted in the recruitment of human myeloid cells into the recipient circulation. Flow cytometry and confocal imaging demonstrated that human bone marrow monocytes and alveolar macrophages in the recipients displayed intact phagocytic function. Human bone marrow-derived monocytes/macrophages were further confirmed to exhibit phagocytosis and killing of *Salmonella typhimurium* upon IFN-γ stimulation. These findings demonstrate the development of mature and functionally intact human myeloid subsets in vivo in the NSG recipients. In vivo human myelopoiesis established in the NSG humanized mouse system may facilitate the investigation of human myeloid cell biology including in vivo analyses of infectious diseases and therapeutic interventions. *The Journal of Immunology*, **2012, 188: 000–000.**

The use of genetically modified mice has led to significant advances in biomedical research by providing insights into the role of individual genes both in normal physiology and in disease pathogenesis. However, translation of these findings into effective therapies for human diseases has been limited by the gap that exists between murine and human biology. The availability of human samples (e.g., cells and tissues), although supporting successful translation from bench research to clinical medicine, is limited by both logistic and ethical concerns.

Therefore, mice repopulated with human hematopoietic cells through xenogeneic transplantation were developed directly to investigate the human immuno-hematopoietic system in vivo. Based on pioneering work using the Hu-PBL-SCID (1) and SCID-hu (2) systems, investigators have aimed to improve xenotransplantation models using immunodeficient strains of mice as recipients of human hematopoietic stem cells (HSCs) to achieve long-term engraftment of multiple human hematopoietic and immune subsets (3). NOD/SCID mice, established by back-crossing the *scid* mutation onto the NOD strain background, are characterized by partially impaired innate immunity and deficient complement-dependent cytotoxicity and are the gold standard for stable human hematopoietic stem/progenitor cell engraftment (3, 4). The ability of NOD-*scid* mice to support human HSC engraftment is associated with a human-like polymorphism in the IgV domain of the signal regulatory protein-α (*Sirpa*) allele in the NOD strain background resulting in the expression of SIRPα with enhanced binding of human CD47 (5). The interaction between SIRPα and CD47 has previously been implicated in the negative regulation of phagocytosis by macrophages through a "do-not-eat-me signal" (6).

The introduction of IL2r common γ-chain mutations onto the NOD/SCID and BALBc/Rag2KO backgrounds led to the generation of the NOD/SCID/γ_c^{null} (NOG) (7, 8) strain with a truncated IL-2Rγ, the NOD/SCID/IL2rγ^{null} (NSG) (9, 10) strain with a complete IL-2Rγ-null mutation, and BALB/c-Rag2KO/γ_c^{null} mice (11), resulting in more profound defects in innate immunity. In vivo human hematopoietic repopulation through transplantation

*Department of Medical Genome Sciences, Graduate School of Frontier Sciences, The University of Tokyo, Chiba, Japan; †Division of Mucosal Immunology, The Institute of Medical Science, The University of Tokyo, Tokyo, Japan; ‡Research Unit for Human Disease Models, RIKEN Research Center for Allergy and Immunology, Yokohama, Japan; §Nippon Becton Dickinson Company, Tokyo, Japan; ¶The Jackson Laboratory, Bar Harbor, ME; and ‖Core Research for Evolutional Science and Technology, Japan Science and Technology Agency, Tokyo, Japan

Received for publication December 30, 2011. Accepted for publication April 19, 2012.

This work was supported by grants from the Ministry of Education, Culture, Sports, Science and Technology of Japan and from the Takeda Science Foundation (to F.I.); grants from the Ministry of Education, Culture, Sports, Science and Technology of Japan (to H.K. and J.K.); the Program for Promotion of Basic and Applied Researches for Innovations in Bio-oriented Industry (to J.K.); and grants from the National Institutes of Health, the U.S. Army Medical Research Institute of Infectious Diseases, and the Helmsley Foundation (to L.D.S.). Y.K. is a Japan Society for the Promotion of Science fellow.

Address correspondence and reprint requests to Fumihiko Ishikawa, Research Unit for Human Disease Models, RIKEN Research Center for Allergy and Immunology, 1-7-22 Suehiro-cho Tsurumi-ku, Yokohama 230-0045, Japan. E-mail address: f_ishika@rcai.riken.jp

The online version of this article contains supplemental material.

Abbreviations used in this article: BM, bone marrow; CB, cord blood; cDC, conventional dendritic cell; DC, dendritic cell; HSC, hematopoietic stem cell; MNC, mononuclear cell; MOI, multiplicity of infection; PB, peripheral blood; pDC, plasmacytoid dendritic cell; rhG-CSF, recombinant human G-CSF; rhGM-CSF, recombinant human GM-CSF; rhIFN-γ, recombinant human IFN-γ; rhM-CSF, recombinant human M-CSF.

www.jimmunol.org/cgi/doi/10.4049/jimmunol.1103660

of human $CD34^+$ or $CD34^+CD38^-$ HSCs in these severely immunocompromised recipients accelerated human stem cell and immunology research by allowing higher levels of human HSC engraftment, differentiation of human T cells in the murine thymus and secondary lymphoid organs, enhanced maturation of human B cells, and human immune function in vivo (7–12).

Despite these advances, one of the remaining issues to be clarified in humanized mouse research has been the development of human myeloid lineage cells in the host mouse tissues. To date, we and others reported the development of human $CD33^+$ myeloid cells and myeloid subsets in NOG mice, BALB/c-Rag2KO/γ_c^{null} mice, and NSG mice (7, 9, 11, 13). In this study, by using NSG newborns as recipients, we present in vivo differentiation of human myeloid subsets in the bone marrow (BM), spleen, and respiratory tract of NSG mice engrafted with purified $lineage^-CD34^+CD38^-$ human cord blood (CB) HSCs. Human granulocytes (neutrophils, basophils, and mast cells) and APCs (monocytes/macrophages, conventional dendritic cells [cDCs] and plasmacytoid dendritic cells [pDCs]) developing in NSG mice exhibited characteristics of human myeloid cells including morphological features and expression of surface molecules known to be associated with the myeloid cell subsets. Moreover, human myeloid cells developing in the NSG recipients displayed functionality such as responsiveness to cytokine or TLR adjuvant and phagocytic function. The in vivo system supporting the development of mature human myeloid cells with intact function will facilitate the evaluation of human myeloid development from hematopoietic stem/progenitor cells, advance in vivo investigation of human myeloid cell-mediated immune responses against pathogens and malignancies, and will support studies of therapeutic agents.

Materials and Methods

Mice

NOD.Cg-*Prkdc*^{scid}*IL2rg*^{tm1Wjl}/Sz (NSG) mice were developed at The Jackson Laboratory by back-crossing a complete null mutation at the *Il2rg* locus onto the NOD.Cg-*Prkdc*^{scid} (NOD/SCID) strain (9, 10). Mice were bred and maintained under defined flora with irradiated food at the animal facility of RIKEN and at The Jackson Laboratory according to guidelines established by the institutional animal committees at each respective institution.

Purification of human HSCs and xenogeneic transplantation

All experiments were performed with authorization from the Institutional Review Board for Human Research at RIKEN Research Center for Allergy and Immunology. CB samples were first separated for mononuclear cells (MNCs) by LSM lymphocyte separation medium (MP Biomedicals). CB MNCs were then enriched for human $CD34^+$ cells by using anti-human CD34 microbeads (Miltenyi Biotec) and sorted for $7AAD^-lineage(hCD3/hCD4/hCD8/hCD19/hCD56)^-CD34^+CD38^-$ HSCs using FACSAria (BD Biosciences). To achieve high purity of donor HSCs, doublets were excluded by analysis of forward scatter-height/forward scatter-width and side scatter-height/side scatter-width. The purity of HSCs was higher than 98% after sorting. Newborn (within 2 d of birth) recipients received 150 cGy total body irradiation using a ^{137}Cs-source irradiator, followed by i.v. injection of 1×10^4–3×10^4 sorted HSCs via the facial vein (14). The recipient peripheral blood (PB) harvested from the retro-orbital plexus was evaluated for human hematopoietic engraftment every 3 to 4 wk starting at 6 wk posttransplantation. At 4–6 mo posttransplantation, recipient mice were euthanized for analysis.

Flow cytometry

Erythrocytes in the PB were lysed with Pharm Lyse (BD Biosciences). Single-cell suspensions were prepared from BM and spleen using standard procedures. To isolate MNCs from the lung, lung tissues were carefully excised, teased apart, and dissociated using collagenase (Wako) (15). The following mAbs were used for identifying engraftment of human hematopoietic cells in NSG recipients: anti-human CD3 V450 (clone UCHT1) and PE–Cy5 (HIT3a), anti-hCD4 PE–Cy5 (RPA-T4), anti-hCD8 PE–Cy5 (RPA-T8), anti-hCD11b/Mac-1 Pacific blue (ICRF44), anti-hCD11c allophycocyanin (B-ly6), anti-hCD14 Alexa700 (M5E2), allophycocyanin–H7 and V450 (MφP9), anti-hCD15 allophycocyanin (HI98) and V450 (MMA), anti-hCD19 PerCP–Cy5.5, PE–Cy5 and PE–Cy7 (SJ25C1), anti-hCD33 PE and PE–Cy7 (p67.6), anti-hCD34 PE–Cy7 (8G12), anti-hCD38 FITC and allophycocyanin (HB7), anti-hCD45, V450 and V500 (HI30), anti-hCD45 AmCyan and allophycocyanin–Cy7 (2D1), anti-hCD56 FITC (NCAM16.2) and PE–Cy5 (B159), anti-hCD114/G-CSFR PE (LMM741), anti-hCD116/GM-CSFR FITC (hGMCSFR-M1), anti-hCD117/c-Kit PerCP–Cy5.5 (104D2), anti-hCD119/IFN-γR PE (GIR-208), anti-hCD123/IL-3R PE and PerCP–Cy5.5 (7G3), anti-hCD284/TLR2 Alexa647 (11G7), anti–HLA-DR allophycocyanin–H7 (L243), anti-mouse CD45 PerCP–Cy5.5 and allophycocyanin–Cy7 (30-F11), all from BD Biosciences; anti-human CD1c/BDCA-1 FITC (AD5-8E7), anti-hCD141/BDCA-3 FITC, PE and allophycocyanin (AD5-14H12), anti-hCD303/BDCA-2 PE (AC144) from Miltenyi; anti-human CD115/M-CSFR PE (9-4D2-1E4), anti-hCD203c/E-NPP3 PE (NP4D6), anti-hCD284/TLR4 PE (HTA125), anti-hFcεRI FITC (AER-37), anti-mouse CD45 Alexa700 (30-F11) from BioLegend. The labeled cells were analyzed using FACSCantoII or FACSAria (BD Biosciences).

Morphological analysis

Cytospin specimens of FACS-purified human myeloid cells were prepared with a Shandon Cytospin 4 cytocentrifuge (Thermo Electric). To identify nuclear and cytoplasmic characteristics of each myeloid cell, cytospin specimens were stained with 100% May–Grünwald solution (Merck) for 3 min, followed by 50% May–Grünwald solution in phosphate buffer (Merck) for an additional 5 min, and then with 5% Giemsa solution (Merck) in phosphate buffer for 15 min. All staining procedures were performed at room temperature. Light microscopy was performed with a Zeiss Axiovert 200 (Carl Zeiss).

In vitro cytokine stimulation and phospho-specific flow cytometry

After 2-h preculture at 37°C in RPMI 1640 (Sigma) containing 10% FBS, recipient BM cells were incubated for 15 min in medium supplemented with 100 ng/ml recombinant human IFN-γ (rhIFN-γ; BD Biosciences), 100 ng/ml recombinant human G-CSF (rhG-CSF; PeproTech), 100 ng/ml recombinant human GM-CSF (rhGM-CSF; PeproTech) or 100 ng/ml recombinant human M-CSF (rhM-CSF; R&D Systems), fixed for 10 min at 37°C with Phosflow Lyse/Fix Buffer (BD Biosciences), permeabilized for 15 min at 4°C with 0.5× Phosflow Perm Buffer IV (BD Biosciences), and labeled using the following set of Abs: anti-human CD3 PerCP–Cy5.5 (SK7), anti-hCD14 PE (M5E2), anti-hCD15 allophycocyanin (HI98), anti-hCD33 PE–Cy7 (p67.6), anti-hCD45 V450 (HI30), anti-mouse CD45 allophycocyanin–Cy7 (30-F11), and the combination of anti-human p-STAT1 Alexa488 (4a), p-STAT3 Alexa488 (4/P-STAT3), p-STAT4 Alexa488 (38/p-Stat4), p-STAT5 Alexa488, and p-STAT6 Alexa488 (18/P-Stat6), all from BD Biosciences. Phosphorylation of STAT molecules was analyzed using FACSCantoII (BD Biosciences). Digital data were converted into a heat map using an online analysis system (Cytobank; http://www.cytobank.org/) (16).

In vivo rhG-CSF treatment of humanized NSG mice

Human CB HSC-engrafted NSG recipients at 4–6 mo posttransplantation were given rhG-CSF (PeproTech) at 300 μg/kg s.c. once a day for five consecutive days. The recipients were analyzed for the frequency of $hCD45^+CD15^+CD33^{low}$ fraction (neutrophils) and $hCD45^+CD15^{-/low}$ $CD33^+$ fraction (monocytes and DCs) before and after rhG-CSF treatment.

In vitro phagocytosis by human myeloid subsets

In vitro phagocytosis was examined using Fluoresbrite Yellow Green carboxylate microspheres (Polysciences). After single-cell preparation, recipient lung and BM cells were precultured for 2 h at 37°C in RPMI 1640 (Sigma) containing 10% FBS then incubated with fluorescent beads (particle/cell ratio = 10:1) for 1 h at 37°C or 4°C and labeled with anti-mouse CD45 allophycocyanin–Cy7, anti-human CD45 allophycocyanin and anti-hCD33 PE–Cy7 (all from BD Biosciences) for identification of fluorescent $beads^+$ $hCD45^+hCD33^+$ cells. The frequencies of observed fluorescent $beads^+$ $hCD45^+hCD33^+$ cells out of total $hCD45^+hCD33^+$ cells were determined. Fluorescent $beads^+$ $hCD45^+hCD33^+$ human lung myeloid cells were purified using FACSAria (BD Biosciences) and imaged using a laser-scanning confocal microscope (Zeiss LSM 710; Carl Zeiss). The intracellular localization of fluorescent beads was confirmed by scanning z-series sections.

TLR analysis and in vivo LPS stimulation of humanized NSG mice

Surface expression levels of TLR2 and TLR4 were analyzed by FACSCantoII. To test the LPS-induced inflammatory response, human CB

HSC-engrafted NSG recipients at 4–6 mo posttransplantation were injected i.v. with LPS at 15 μg/mouse. After LPS injection, plasma was collected from 0 to 4 h. Human cytokines IL-1β, IL-6, IL-8, IL-10, IL-12p70, and TNF were measured by cytometric bead array (BD Biosciences).

IFN-γ–induced Salmonella *killing activity by humanized mouse-derived monocytes/macrophages*

Salmonella typhimurium PhoPc strain transformed with the pKKGFP plasmid was kindly provided by J.P. Kraehenbuhl (17). *S. typhimurium* was grown shaking at 180 rpm overnight in Luria–Bertani broth supplemented with 100 μg/ml ampicillin at 37°C. BM monocytes/macrophages were purified by FACSAria (BD) based on the phenotypic characterization of lineage (CD3, CD7, CD16, CD19, CD56, CD123, CD235a)-negative, mouse CD45 and Ter119-negative, human $CD45^+CD11b^+$. Aliquots of (10^4) human monocytes/macrophages derived from humanized mouse BM were cultured on collagen type I-coated 96-well plates (BD) for 24 h in either the presence or the absence of 1000 U/ml recombinant human IFN-γ (BD). Then, cells were infected with *S. typhimurium* at multiplicity of infection (MOI) of 20 at 37°C for 2 h, and the infection was confirmed by fluorescence microscopy (Biorevo BZ-9000; Keyence). For intracellular CFU determination, cells were washed twice with PBS and lysed in 0.2% Triton X-100 in PBS for 2 min, and lysates were diluted and plated onto Luria–Bertani broth agar plates containing 100 μg/ml ampicillin for colony enumeration.

Statistical analysis

The numerical data are presented as means ± SEM unless otherwise noted. Where noted, two-tailed *t* tests were performed, and the differences with the *p* value <0.05 were deemed statistically significant (GraphPad Prism; GraphPad).

Results

Human myeloid lineage cells develop in NSG mice transplanted with human CB HSCs

Recent advances in our knowledge of innate immunity reemphasize the importance of myeloid cells for sensing, capturing, and processing Ags for the initiation of innate and acquired phases of immune responses. The development of human myeloid cells in HSC-engrafted NSG mice has not previously been studied in detail. To evaluate in vivo differentiation and function of human myeloid lineage cell populations, we transplanted 1×10^4–3×10^4 purified human $lineage^-CD34^+CD38^-$ CB HSCs intravenously into sublethally irradiated newborn NSG mice. At 4–6 mo posttransplantation, we confirmed high levels of human hematopoietic chimerism and multilineage differentiation of human immune subsets as evidenced by flow cytometry (Fig. 1A, 1B). In addition to the reconstitution of human adaptive immunity ($CD3^+$ T cells and $CD19^+$ B cells), we identified the development of human innate immune cell subsets such as $CD56^+$ NK cells and $CD33^+$ myeloid cells in the recipient mice. The frequency of human myeloid lineage cells was higher in the recipient BM (30.7 ± 3.9%, $n = 11$) compared with that in the spleen (6.2 ± 1.2%, $n = 11$, $p < 0.0001$ by paired two-tailed *t* test) and PB (7.1 ± 1.3%, $n = 11$, $p < 0.0003$) (Fig. 1B).

We then identified the subsets of human myeloid cells present in the humanized NSG recipient mice through flow cytometry. Human myeloid subsets are classified into HLA class II-negative granulocytes and class II-positive APCs. In the BM and spleen

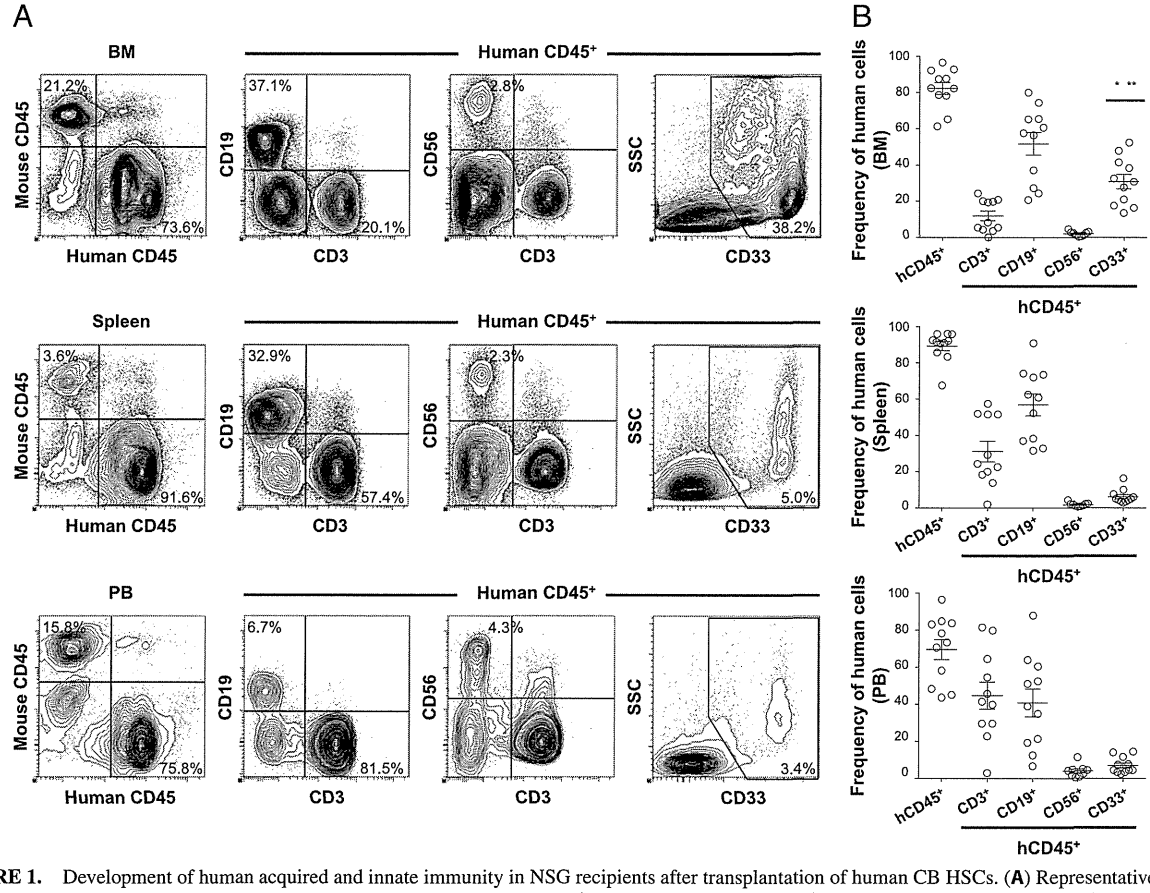

FIGURE 1. Development of human acquired and innate immunity in NSG recipients after transplantation of human CB HSCs. (**A**) Representative sets of flow cytometry contour plots demonstrating the development of human $CD45^+$ hematopoietic cells, $hCD3^+$ T cells, $hCD19^+$ B cells, $hCD56^+$ NK cells, and $hCD33^+$ myeloid cells in the BM, spleen, and PB of an NSG recipient. (**B**) Human $CD45^+$ hematopoietic chimerism and the frequencies of $hCD3^+$ T, $hCD19^+$ B, $hCD33^+$ myeloid cells ($n = 11$ each, frequency of myeloid cells in BM compared with spleen, $^*p < 0.0001$, and with PB, $^{**}p < 0.0003$) and $hCD56^+$ NK ($n = 9$ each) cells in the BM, spleen, and PB of NSG recipients at 4–6 mo posttransplantation are summarized.

of NSG recipients at 4–6 mo posttransplantation, we observed differentiation of both human granulocytes and APCs. Among the granulocyte lineage, human $CD15^+CD33^{low}HLA\text{-}DR^-$ neutrophils, $CD117^-CD123^+CD203c^+$ basophils, and $CD117^+CD203c^+HLA\text{-}DR^-$ mast cells were observed in the recipient BM and spleen. Analyses of APC populations found that $CD14^+CD33^+HLA\text{-}DR^+$

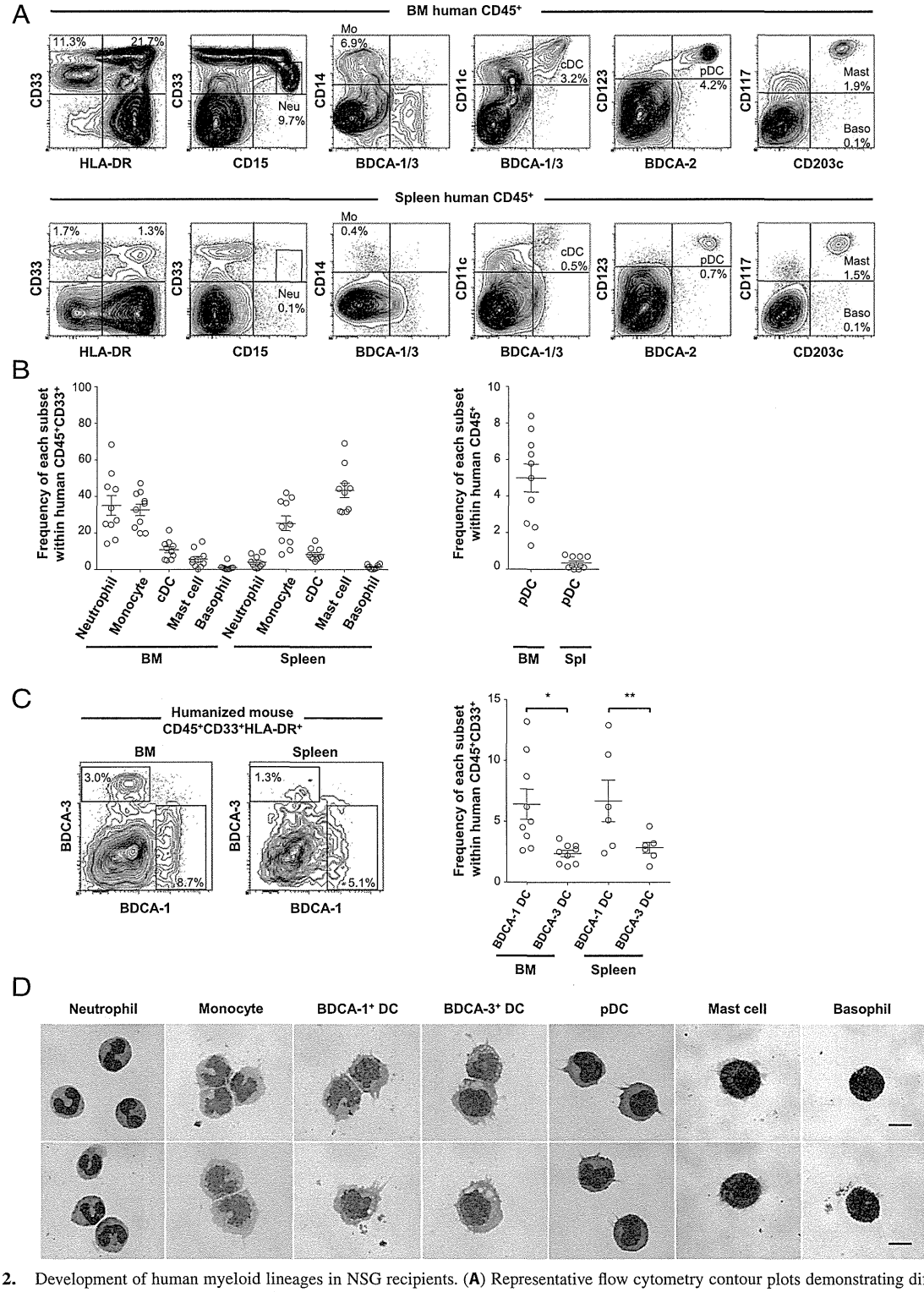

FIGURE 2. Development of human myeloid lineages in NSG recipients. (**A**) Representative flow cytometry contour plots demonstrating differentiation of human $HLA\text{-}DR^-$ granulocytes and $HLA\text{-}DR^+$ APCs in the BM and spleen of an NSG recipient. (**B**) The frequencies of human neutrophils, monocytes, cDCs, mast cells, basophils, and pDCs in the BM and spleen of NSG recipients are summarized ($n = 10$). (**C**) In the humanized mouse BM and spleen, two distinct subsets of DCs, $BDCA\text{-}1^+$ DCs and $BDCA\text{-}3^+$ DCs, were identified in $HLA\text{-}DR^+CD33^+CD11c^+$ conventional DCs. Frequencies of the two DC subsets within BM and spleen $hCD45^+CD33^+$ cells are shown (BM, $n = 9$, $^*p = 0.007$, significant differences between cDCs; spleen, $n = 6$, $^{**}p = 0.046$). (**D**) Human myeloid cells isolated by cell sorting of recipient BM demonstrate characteristic morphological features on May–Grünwald–Giemsa stain. Baso, Basophils; Mast, mast cells; Mo, monocytes; Neu, neutrophils. Scale bars, 10 μm.

BDCA-1$^-$BDCA-3$^-$ monocytes, CD14$^-$CD33$^+$HLA-DR$^+$BDCA-1$^+$ or BDCA-3$^+$ cDCs, and CD123$^+$BDCA-2$^+$HLA-DR$^+$ pDCs developed in the recipients BM and spleen (Fig. 2A, 2B). The frequency of CD15$^+$CD33^{low}HLA-DR$^-$ neutrophils within human CD45$^+$CD33$^+$ myeloid cells were present at the highest level in the BM (35.0 ± 5.4%, n = 10), whereas CD117$^+$CD203c$^+$FcεRI^{low} HLA-DR$^-$ mast cells developed at a higher efficiency in the recipient spleen (43.3 ± 4.0% within CD45$^+$CD33$^+$, n = 10) (Fig. 2B). Among human APCs developing in the NSG recipients, monocytes accounted for the highest frequency in total myeloid cells both in the BM (32.6 ± 3.1%, n = 10) and spleen (25.2 ± 4.0%, n = 10). cDCs are divided into two subsets according to the expression of BDCA-1 and BDCA-3. Within human CD45$^+$CD33$^+$ myeloid cells, the frequencies of BDCA-1$^+$ DCs accounted for 6.4 ± 1.2% in BM (n = 9) and 6.7 ± 1.7% in spleen (n = 6) and were significantly higher than those of BDCA-3$^+$ DCs (2.4 ± 0.3% and 2.8 ± 0.4%, respectively) (Fig. 2C). We then performed flow cytometric analysis using the same mAbs to determine the frequencies of each myeloid subset in primary BM MNCs. Although we could not directly compare human neutrophil development, the proportion of human monocytes, BDCA1$^+$ cDCs, BDCA3$^+$ cDCs, and pDCs was similar between primary human BM and humanized mouse BM (Supplemental Fig.1). In addition to the expression analysis of cell surface molecules, we performed May–Grünwald–Giemsa staining to identify the morphology of the myeloid lineage cells developing in the NSG recipients. Human myeloid cells purified from NSG recipient BM exhibited characteristic morphological features (Fig. 2D).

Human myeloid lineage cells developing in NSG recipients demonstrate intact functional responses to human cytokines in vitro and in vivo

We confirmed the development of various human myeloid subsets in the BM and spleen of NSG recipients and next examined the expression of human cytokine receptors including IFN-γR, G-CSFR, GM-CSFR, and M-CSFR compared with that in human CB (Fig. 3A–C). By using human CD45$^+$CD33$^+$ CB myeloid cells as control, we confirmed that human CD45$^+$CD33$^+$ cells in the recipient BM expressed comparable levels of IFN-γR, G-CSFR, GM-CSFR and M-CSFR (n = 5, no significant difference between humanized mouse BM and CB, p = 0.6444, p = 0.0985, p = 0.3879, and p = 0.5816, respectively) (Fig. 3D).

To demonstrate functional responses to human cytokine stimulation at a cellular level, we examined the phosphorylation of STAT molecules using flow cytometry. Recent studies have revealed that hematopoietic cytokine receptor signaling is largely mediated by JAK kinases and STAT molecules known as the downstream transcription factors (18). BM cells from NSG recipients (n = 3) were

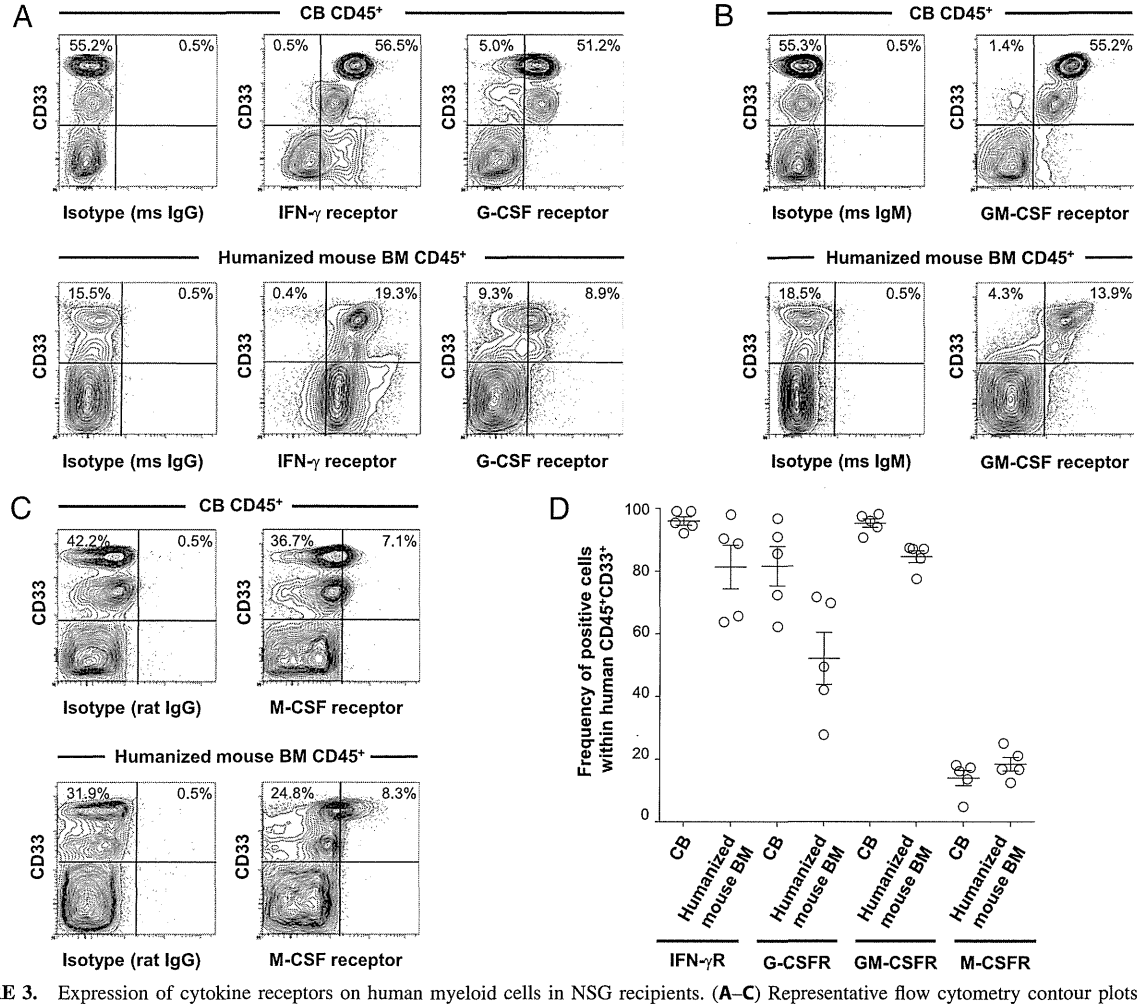

FIGURE 3. Expression of cytokine receptors on human myeloid cells in NSG recipients. (**A–C**) Representative flow cytometry contour plots demonstrating the expression of IFN-γR, G-CSFR, GM-CSFR, and M-CSFR by CB hCD45$^+$CD33$^+$ myeloid cells (top) and by hCD45$^+$CD33$^+$ myeloid cells derived from humanized NSG BM (bottom). Contour plots for isotype control Ig are also shown. (**D**) Expression of each cytokine receptor within hCD45$^+$CD33$^+$ cells is summarized (CB, n = 5; humanized NSG BM, n = 5).

stimulated with rhIFN-γ, rhG-CSF, rhGM-CSF, or rhM-CSF in vitro for 15 min at 37°C. In neutrophils and monocytes, rhGM-CSF specifically induced STAT5 phosphorylation, but not irrelevant STATs (e.g., STAT4 and STAT6) (Fig. 4A, 4C). Additionally, rhIFN-γ and rhG-CSF induced optimal STAT phosphorylation (Fig. 4B, 4D, 4E). Indeed, rhIFN-γ stimulation resulted in intracellular STAT1, STAT3, and STAT5 phosphorylation, and rhG-CSF stimulation induced STAT3 and STAT5 phosphorylation, respectively (Fig. 4E). These results indicate that intact molecular events occur in human neutrophils and monocytes in response to recombinant human cytokines in vitro.

We next investigated in vivo cytokine response by human myeloid cells in the NSG humanized mice. Stimulation with rhG-CSF in vivo is known to induce proliferation of myeloid precursors and mobilization of myeloid subsets from BM (19). After in vivo treatment of humanized mice by rhG-CSF for 5 d, the frequencies of $hCD45^+CD15^+CD33^{low}$ fraction (human neutrophils) and $hCD45^+CD15^{-/low}CD33^+$ fraction (human monocytes and DCs) increased in the PB (three out of three recipients) (Fig. 4F). These findings indicate that human myeloid cells developing in the humanized NSG recipients demonstrate functional cytokine response both in vivo and in vitro.

Human inflammatory response via TLR signaling

Along with the role of cytokine receptor signaling in development and function of myeloid cells, signaling via TLRs serves fundamental roles in evoking systemic inflammatory response by myeloid cells (20). We therefore analyzed the expression of TLRs in human myeloid cells developed in the engrafted NSG recipients by flow cytometry. We examined the surface expression of TLR2 and TLR4 in the human myeloid cells developed in the humanized mouse BM. TLR2 is specifically expressed in human monocytes and $BDCA1^+$ DCs, and TLR4 is expressed in the four distinct myeloid subsets, neutrophils, monocytes, $BDCA1^+$ cDCs, and $BDCA3^+$ cDCs (Fig. 5A, 5B). The expression of TLR4 was also confirmed in humanized mouse BM-derived monocytes and other myeloid subsets, which has led us to investigate the in vivo response of human innate immunity against LPS, a potent TLR4

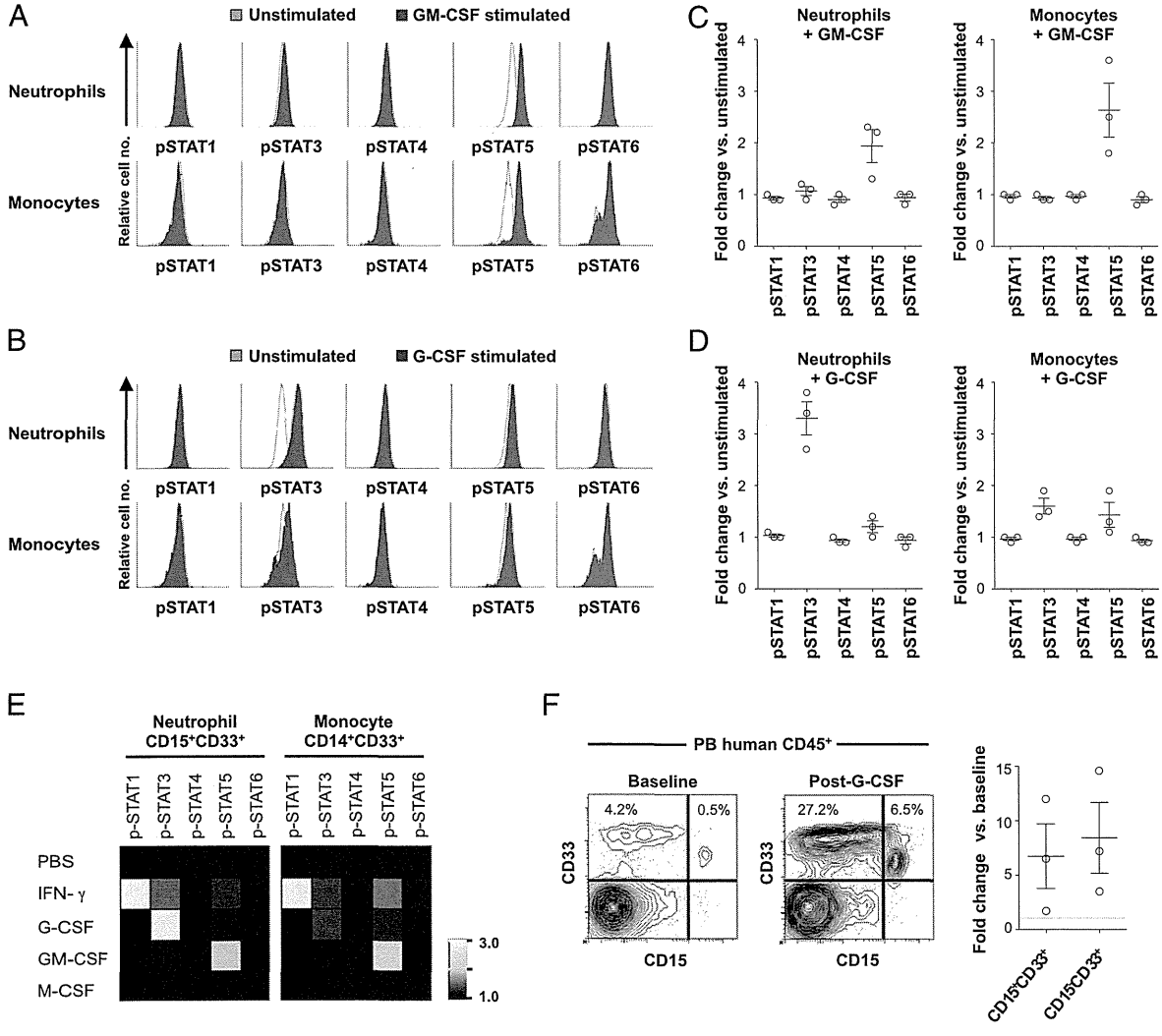

FIGURE 4. Human myeloid lineage cells developing in NSG recipients demonstrate cytokine responses in vitro and in vivo. (**A** and **B**) Phosphorylation of STAT1, STAT3, STAT4, STAT5, and STAT6 in human neutrophils and monocytes derived from an NSG recipient BM after in vitro stimulation with rhGM-CSF (A) and with rhG-CSF (B) was measured by flow cytometry. (**C** and **D**) Results from three independent experiments using three different recipients are summarized. (**E**) Heat map representation of STAT phosphorylation in human neutrophils and monocytes in an NSG recipient BM after in vitro cytokine treatment relative to PBS exposure is shown. (**F**) Representative flow cytometry contour plots demonstrating expansion of myeloid lineage cells in the PB of an NSG recipient in response to in vivo rhG-CSF administration. Frequencies of $hCD45^+CD15^+CD33^{low}$ and $hCD45^+CD15^{-/low}CD33^+$ myeloid cells were increased after in vivo rhG-CSF treatment in PB of NSG recipients for 5 d.

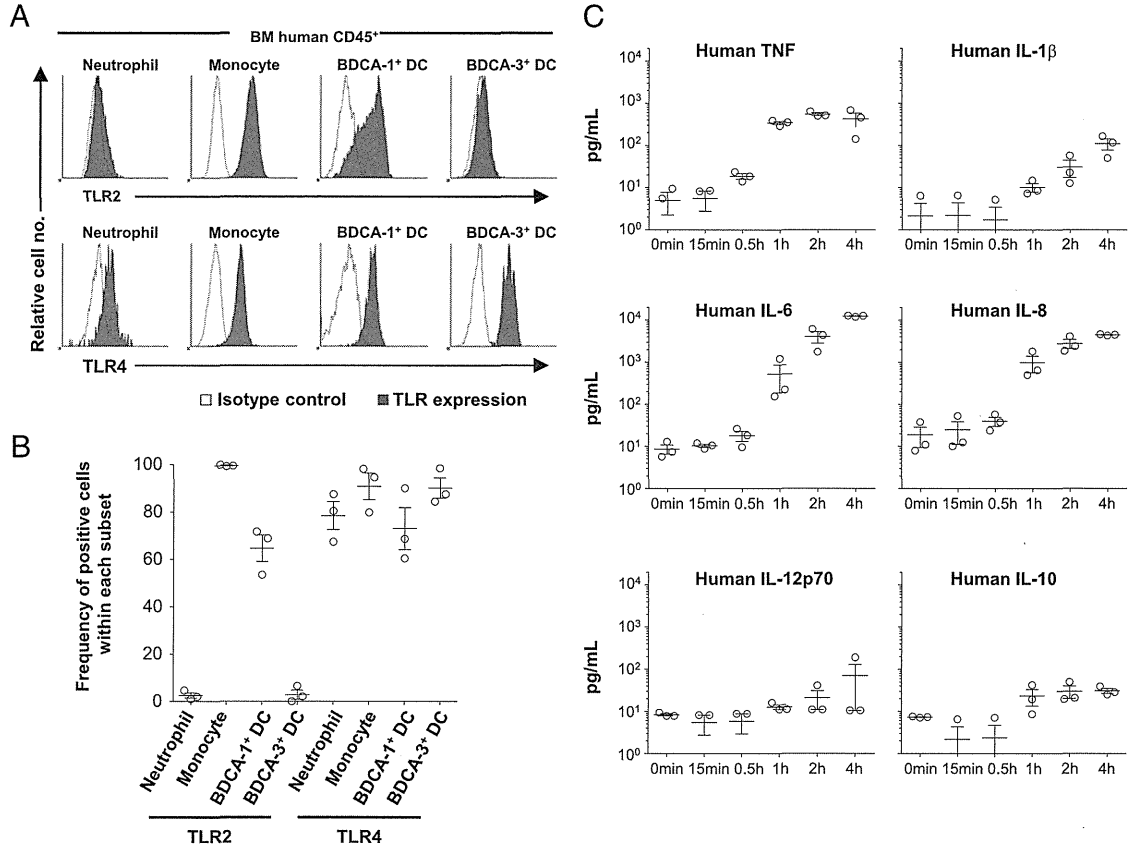

FIGURE 5. Expression of TLRs and response to TLR adjuvant by humanized mouse-derived myeloid subsets. TLR expression is analyzed in the granulocytes, monocytes, and cDCs derived from the humanized NSG recipient BM. (**A** and **B**) Expression of TLR2 and TLR4 in neutrophils, monocytes, BDCA-1$^+$ DCs, and BDCA-3$^+$ DCs was analyzed by flow cytometry. (**C**) At different time points after the injection of 15 μg LPS into humanized NSG recipients, human-specific cytokine levels in plasma were evaluated by cytometric bead array (n = 3).

ligand and endotoxin. To this end, we have administered 15 μg LPS to NSG humanized mice followed by detection of human inflammatory cytokines by flow cytometry. Bead-attached Abs for human cytokines did not detect 5000 pg/ml of mouse cytokines demonstrating that these Abs and analyses are human-specific (Supplemental Fig. 2). Of the cytokines examined, we have seen the significant elevation of plasma levels of human IL-6, human IL-8, and human TNF (Fig. 5C). Time-dependent kinetics showed that the prompt response of human innate cells to the LPS was achieved between 30 min and 1 h after injection. Consequently, humanized mice could be used to examine human innate immune response against infectious organisms and to predict inflammatory response provoked by the TLR ligands.

Human myeloid cells present in NSG recipient lung exhibit functional phagocytosis

In the human immune system, myeloid cells serve an important role in immune surveillance not only in the systemic immune compartments but also in the mucosal tissues, especially the respiratory compartment of lung protected by both mucosal and systemic immune systems (21, 22). To examine whether functional reconstruction of human myeloid cells occurs in the lung, we evaluated the differentiation and function of human myeloid lineage cells isolated from the lungs of NSG recipients. Among human CD45$^+$ cells present in the NSG recipient lung, myeloid lineage cells constituted 20.3 ± 3.8% (n = 8; a representative set of flow cytometry plots shown in Fig. 6A). The majority of human myeloid lineage cells residing in the recipient lungs were CD33$^+$ CD14$^+$HLA-DR$^+$ monocytes/macrophages (60.9 ± 5.1% within huCD45$^+$CD33$^+$, n = 8) (Fig. 6B).

The respiratory tract represents a major port of entry for inhaled pathogenic organisms, and resident alveolar monocytes/macrophages play a major role in surveillance and immune defense. To confirm the phagocytic function of human monocytes/macrophages present in the lungs of NSG recipients, we performed in vitro phagocytosis assay using yellow-green fluorescent beads by flow cytometry and confocal microscopy imaging. After in vitro incubation of NSG recipient-derived human CD45$^+$ cells with 1 and 2 μm fluorescent beads at 37°C, uptake of beads was noted in 9.0 and 7.9% of hCD45$^+$CD33$^+$ human myeloid cells, respectively (Fig. 6C). It should be noted that uptake of fluorescent beads was observed only in hCD45$^+$CD33$^+$ myeloid cells, but not in hCD45$^+$CD33$^-$ lymphoid cells (Fig. 6C). This demonstrates that the fluorescent bead uptake specifically represents phagocytotic function by human lung myeloid cells, not nonspecific uptake of the beads or binding or coating of the cells by the beads. The efficiency of uptake was 24.4 ± 3.0% in the lung-derived hCD45$^+$CD33$^+$ cells (n = 6, p = 0.001 compared with 4°C incubation by two-tailed t test), equivalent to that in BM-derived hCD45$^+$CD33$^+$ cells (16.6 ± 2.7%, n = 4, p = 0.01 compared with 4°C incubation by two-tailed t test) (Fig. 6C, 6D).

Next, phagocytosis of fluorescent beads by human myeloid cells was confirmed by direct visualization by confocal microscopy. Three-dimensional confocal imaging demonstrated intracellular localization of the fluorescent bead signal in sorted fluorescent bead (YG signal)$^+$hCD45$^+$CD33$^+$ human myeloid cells, confirming the

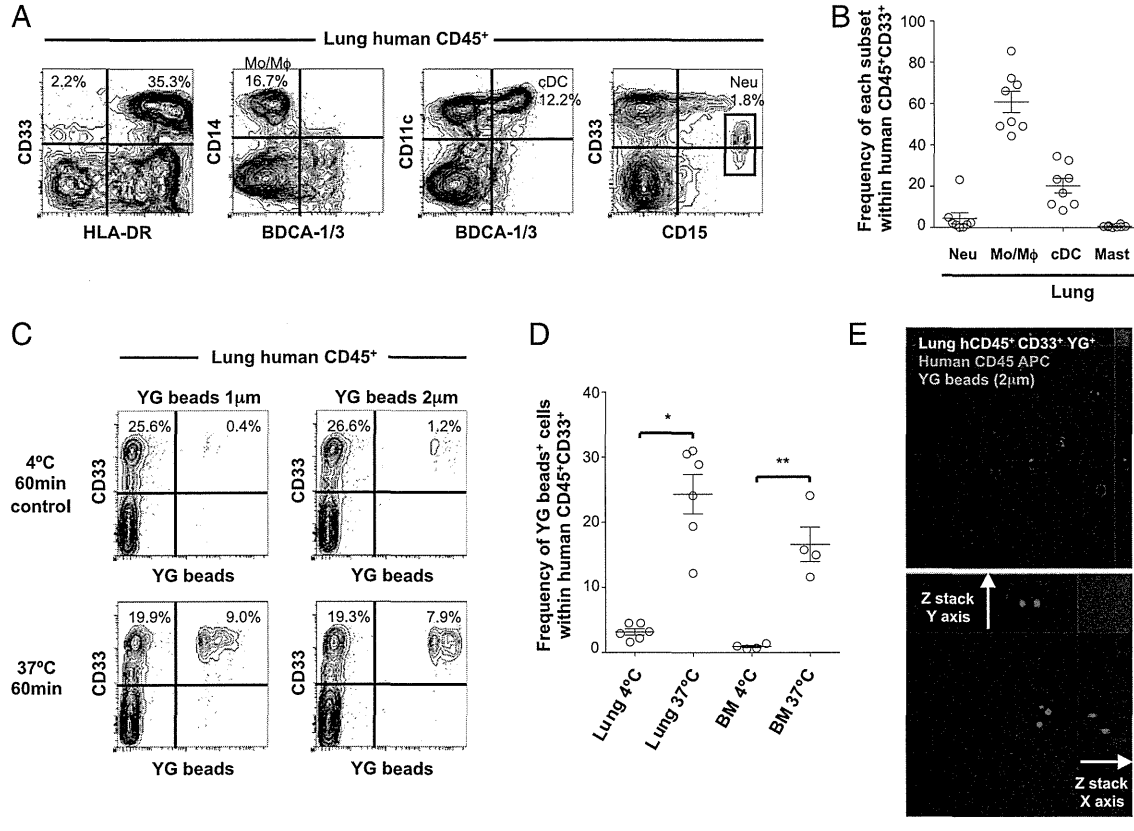

FIGURE 6. Human monocytes/macrophages developing in NSG recipient lung demonstrate phagocytosis of microparticles. (**A**) Representative contour plots demonstrating the reconstitution of human myeloid cells in the lungs of an NSG recipient. Human CD45$^+$ cells within lung cell populations were analyzed by CD33, HLA-DR, CD14, CD11c, BDCA-1/3, and CD15 to identify monocytes/macrophages, cDCs, and neutrophils. (**B**) The frequencies of human neutrophils, monocytes/macrophages, cDCs, mast cells, and basophils within hCD45$^+$CD33$^+$ NSG recipient lung are summarized (n = 8). (**C**) A set of representative flow cytometry plots demonstrating the presence of hCD45$^+$CD33$^+$fluorescent beads$^+$ cells. (**D**) Summary of the frequency of hCD45$^+$ CD33$^+$fluorescent bead$^+$ cells in NSG recipient lung cell populations incubated at 37°C and at 4°C (control), respectively, with fluorescent beads (lung, n = 6; BM, n = 4; *p = 0.001, **p = 0.01). (**E**) Confocal imaging of FACS-purified hCD45$^+$CD33$^+$fluorescent beads$^+$ cells derived from NSG recipient lung cell populations show internalization of fluorescent beads (green) within hCD45 (purple)-expressing human myeloid cells. Baso, Basophils; Mast, mast cells; Mo/Mϕ, monocytes/macrophages; Neu, neutrophils.

internalization of microparticles by human monocytes/macrophages (Fig. 6E). Taken together, these findings demonstrate the presence of human innate immunity with intact phagocytic function in the NSG recipient lung.

Humanized mouse BM-derived monocytes/macrophages exhibit IFN-γ–induced phagocytosis and killing against Salmonella typhimurium

Myeloid subsets serve essential roles in host defense against various infectious microorganisms as a part of innate immunity. Of the various myeloid subsets discussed in the current study, monocytes and macrophages display excellent phagocytic potential by phagolysosome formation, by the effects of oxidative and nitrosative stress, and by antimicrobial cationic peptides and enzymes (23). To evaluate future application of the humanized mouse system in infectious disease research, we examined the phagocytic function of human monocytes/macrophages derived from humanized NSG BM against *S. typhimurium*. We purified mCD45$^-$TER119$^-$hCD45$^+$ Lin$^-$CD11b$^+$ cells as monocytes/macrophages from the recipient BM (Fig. 7A) and cultured 10,000 purified human monocytes/macrophages with *S. typhimurium* at an MOI of 20 with or without prestimulation of human recombinant IFN-γ at 1000 U/ml. In the five in vitro experiments, stimulation of human monocytes/macrophages with rhIFN-γ resulted in the significantly potentiated phagocytosis and killing of *Salmonella* by the humanized mouse-derived monocytes/macrophages as evidenced by the decreased numbers of colony formation by *S. typhimurium* (at 3 h postinfection p = 0.023, at 12 h postinfection p = 0.091 [n.s.] compared with control versus IFN-γ stimulation by two-tailed t test) (Fig. 7B). Taken together, human monocytes that develop in the humanized NSG mice possess phagocytic activity against microbeads and bacteria and kill phagocytized bacteria presumably via signaling through cytokine receptors and TLRs.

Discussion

In vivo reconstitution of mature and functional human myeloid cells not only facilitates in vivo examination of human innate immunity but also offers a promising platform for translational research in the areas of infectious immunity and drug development. In the current study, we have aimed to clarify how functional human myeloid cells develop in NSG humanized mice.

In the NSG recipients, we found distinct levels of reconstitution of myeloid subsets in the BM and spleen. The differential myeloid reconstitution in the humanized hematopoietic organs is comparable to that seen in the human tissues, reflecting the distinct physiological roles of each hematopoietic organ in mammals. BM acts an essential reservoir of short-lived neutrophils and monocytes that readily migrate into sites of infection and inflammation. In addition, BM neutrophils function as paracrine regulators for mobi-

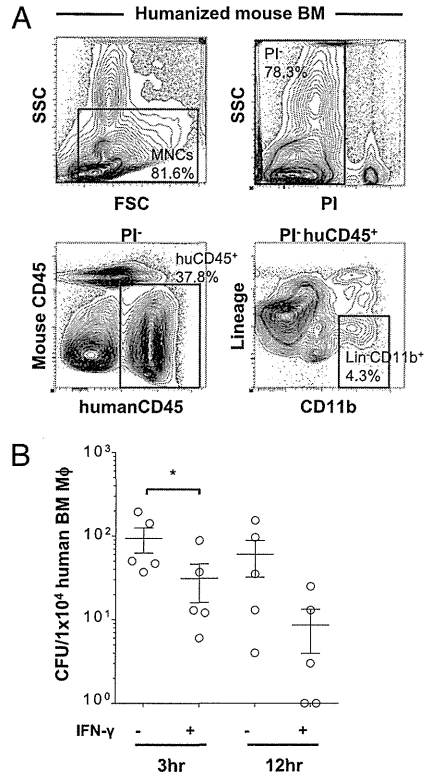

FIGURE 7. Cytotoxicity against *S. typhimurium* by IFN-γ–activated human monocytes/macrophages developing in NSG recipient. (**A**) Within mononuclear cell gate, propidium iodide$^-$ viable, hCD45$^+$Lin$^-$CD11b$^+$ cells were purified from the BM of humanized NSG recipients. Purified BM monocytes/macrophages were stimulated with or without supplementation of 1000 U/ml human IFN-γ for 24 h and then infected with *S. typhimurium* at MOI 20. (**B**) Intracellular CFU was counted at 3 and 12 h postinfection (n = 5, *p = 0.023 compared with nonstimulated).

lization of HSCs via proteases, such as matrix metalloproteinase-9 (MMP9 or gelatinase B), cathepsin G, and neutrophil elastase contained within intracellular granules. The spleen, a major secondary lymphoid organ, is not only the site of B cell maturation and APC interactions with T and B cells but also is an organ supporting the development of mast cells from their progenitors (24, 25). Cross-reactivity of murine stem cell factor with human c-Kit$^+$ cells may explain the high frequency of human mast cells observed in the recipient spleen (26).

The development of human myeloid lineages is regulated by various cytokine signals (18, 27). In the current study, we directly compared the frequencies of human myeloid subsets using humanized mouse BM and primary human BM MNCs. As to the development of human APCs, humanized mouse BM recapitulates physiological development of human monocytes and two different subtypes of cDCs. However, we could not directly compare the frequencies of human neutrophils between humanized mouse BM and primary human BM, as we have used frozen BM MNCs. According to the previous reports, the frequency of human neutrophils in the humanized mouse BM is lower than that in the primary human BM (28, 29).

Human myelopoiesis within the mouse microenvironment may occur through multiple cooperative mechanisms. First, mouse cytokines such as stem cell factor, FLT3 ligand, G-CSF, and thrombopoietin may directly stimulate human myelopoiesis by cross-reacting with their respective receptors on human hematopoietic stem and/or myeloid progenitor cells. These human myeloid cells in turn produce cytokines such as GM-CSF and IL-3, resulting in the differentiation, maturation, and maintenance of human granulocytes, monocytes, and DCs. At the same time, the cytokine milieu within the NSG recipient repopulated with human hematopoietic cells may not be completely sufficient, to support human hematopoiesis as evidenced by the relative paucity of human neutrophils in the recipient BM, spleen, and circulation that might suggest the requirement of human cytokine or adhesion molecules in the hematopoietic tissues of the recipients. Recent studies suggested that the induced expression of human cytokines in the mouse environment may lead to enhanced differentiation and maturation of human myeloid subsets including neutrophils (30–33). In the current study, however, human monocytes develop in NSG recipients despite the fact that M-CSF is exclusively produced in non-hematopoietic cells and that murine M-CSF does not cross-react with human M-CSFR. This may be attributable to the redundancy among cytokines such as M-CSF, GM-CSF, and IL-3 as demonstrated in previous studies using M-CSF–deficient mice (34).

As a measure of human myeloid cell function, we investigated cytokine responses in human neutrophils and monocytes developing in the NSG recipients. Consistent with the expression of cytokine receptors identified on the human myeloid cells, neutrophils and monocytes showed intact responses to human cytokines both in vivo and in vitro. Phosphorylation of STAT molecules represents a molecular event downstream of cytokine receptor activation. STAT1 is a key mediator of IFN-γ activation of cells and an indispensable component of IFN-γ–dependent innate defense mechanisms against infections (35). The STAT3 signaling pathway is essential for G-CSF–mediated granulopoiesis (36). Specific phosphorylation of STAT5 may be an essential molecular event enabling generation of granulocytes from myeloid progenitors and proliferation and survival of mature neutrophils (37). STAT4 and STAT6 are essential for mediating IL-12 and IL-4 signaling in Th cells (38, 39). Human myeloid cells developing in humanized NSG recipients responded to human cytokines in a specific manner, as determined by the selective activation of JAK–STAT signaling pathways to corresponding cytokines.

Similar to the analysis of the expression of cytokine receptors and signaling, we showed that human myeloid subsets developing in the NSG humanized mice expressed various TLRs at the protein level. In the analysis of TLR expression in humanized mouse BM-derived cells, specific expression of TLR2 was observed in human monocytes and BDCA1$^+$ cDCs rather than neutrophils or BDCA3$^+$ cDCs. Consistent with the expression of TLR4 in human myeloid subsets, in vivo administration of LPS provoked a potent human inflammatory response as demonstrated by the prompt elevation of plasma hIL-6, hIL-8, and hTNF levels. In addition to the examination of cytokine and TLR signaling in human myeloid cells, we investigated the function of human myeloid cells against bacteria to elucidate whether the humanized mouse system can be applied to the research for infectious immunity. As an example of bacterial infection, we chose *S. typhimurium*, a Gram-negative bacillus causing gastrointestinal infections and invasive diseases, especially in children and immunosuppressed patients (40). IFN-γ mediates signaling to activate monocytes and macrophages in phagocytosis (41, 42). In the analysis of colony formation by *S. typhimurium*, IFN-γ potentiated the phagocytosis and antimicrobial activities of humanized mouse BM-derived monocytes/macrophages against this microorganism.

We observed not only systemic reconstitution of human myeloid subsets but also development of respiratory mucosal immunity in NSG humanized mice. Recent mouse studies revealed the crucial and specific roles of mucosal immunity in immune surveillance and

immunological homeostasis in the respiratory tracts (21, 22). In the recipient lung, unlike the BM or spleen, $CD33^+CD14^+HLA\text{-}DR^+$ macrophages were the predominant myeloid population. Frequencies of human B cells, T cells, and myeloid cells in the recipient lung were distinct from those in the recipient PB, excluding the possibility that the human myeloid cells isolated from the recipient lung are contaminating PB myeloid cells. Importantly, macrophages, the predominant human myeloid subset in the recipient lung, demonstrated intact phagocytic function. Macrophages in the NSG recipients will be compared with the recently reported hGM-CSF and hIL-3 knock-in Rag2KO/IL2rγKO humanized mice showing abundant human macrophages in bronchoalveolar lavage (32). Establishment of an in vivo model of human pulmonary mucosal immunity may enable investigation of in vivo immune surveillance in the respiratory tract and in allergic pulmonary disorders and may allow evaluation of vaccines at preclinical stages (43, 44).

In this study, the reconstitution of both systemic and mucosal human innate immunity was observed in the NSG humanized mice. We performed phenotypic characterization and functional evaluation of human myeloid cells developing in the recipients, including granulocytes and APCs. Humanized mice reconstituted with both lymphoid and myeloid human lineages would facilitate in vivo investigation of interactions between the lymphoid and the myeloid compartments, allowing the dissection of the coordinated human immune response at the level of the whole organism.

Disclosures

The authors have no financial conflicts of interest.

References

1. Mosier, D. E., R. J. Gulizia, S. M. Baird, and D. B. Wilson. 1988. Transfer of a functional human immune system to mice with severe combined immunodeficiency. *Nature* 335: 256–259.
2. McCune, J. M., R. Namikawa, H. Kaneshima, L. D. Shultz, M. Lieberman, and I. L. Weissman. 1988. The SCID-hu mouse: murine model for the analysis of human hematolymphoid differentiation and function. *Science* 241: 1632–1639.
3. Greiner, D. L., R. A. Hesselton, and L. D. Shultz. 1998. SCID mouse models of human stem cell engraftment. *Stem Cells* 16: 166–177.
4. Shultz, L. D., P. A. Schweitzer, S. W. Christianson, B. Gott, I. B. Schweitzer, B. Tennent, S. McKenna, L. Mobraaten, T. V. Rajan, D. L. Greiner, et al. 1995. Multiple defects in innate and adaptive immunologic function in NOD/LtSz-scid mice. *J. Immunol.* 154: 180–191.
5. Takenaka, K., T. K. Prasolava, J. C. Wang, S. M. Mortin-Toth, S. Khalouei, O. I. Gan, J. E. Dick, and J. S. Danska. 2007. Polymorphism in Sirpa modulates engraftment of human hematopoietic stem cells. *Nat. Immunol.* 8: 1313–1323.
6. Oldenborg, P. A., A. Zheleznyak, Y. F. Fang, C. F. Lagenaur, H. D. Gresham, and F. P. Lindberg. 2000. Role of CD47 as a marker of self on red blood cells. *Science* 288: 2051–2054.
7. Hiramatsu, H., R. Nishikomori, T. Heike, M. Ito, K. Kobayashi, K. Katamura, and T. Nakahata. 2003. Complete reconstitution of human lymphocytes from cord blood CD34+ cells using the NOD/SCID/gammacnull mice model. *Blood* 102: 873–880.
8. Ito, M., H. Hiramatsu, K. Kobayashi, K. Suzue, M. Kawahata, K. Hioki, Y. Ueyama, Y. Koyanagi, K. Sugamura, K. Tsuji, et al. 2002. NOD/SCID/gamma (c)(null) mouse: an excellent recipient mouse model for engraftment of human cells. *Blood* 100: 3175–3182.
9. Ishikawa, F., M. Yasukawa, B. Lyons, S. Yoshida, T. Miyamoto, G. Yoshimoto, T. Watanabe, K. Akashi, L. D. Shultz, and M. Harada. 2005. Development of functional human blood and immune systems in NOD/SCID/IL2 receptor gamma chain(null) mice. *Blood* 106: 1565–1573.
10. Shultz, L. D., B. L. Lyons, L. M. Burzenski, B. Gott, X. Chen, S. Chaleff, M. Kotb, S. D. Gillies, M. King, J. Mangada, et al. 2005. Human lymphoid and myeloid cell development in NOD/LtSz-scid IL2R gamma null mice engrafted with mobilized human hemopoietic stem cells. *J. Immunol.* 174: 6477–6489.
11. Traggiai, E., L. Chicha, L. Mazzucchelli, L. Bronz, J. C. Piffaretti, A. Lanzavecchia, and M. G. Manz. 2004. Development of a human adaptive immune system in cord blood cell-transplanted mice. *Science* 304: 104–107.
12. Legrand, N., K. Weijer, and H. Spits. 2006. Experimental models to study development and function of the human immune system in vivo. *J. Immunol.* 176: 2053–2058.
13. McDermott, S. P., K. Eppert, E. R. Lechman, M. Doedens, and J. E. Dick. 2010. Comparison of human cord blood engraftment between immunocompromised mouse strains. *Blood* 116: 193–200.
14. Ishikawa, F., A. G. Livingston, J. R. Wingard, S. Nishikawa, and M. Ogawa. 2002. An assay for long-term engrafting human hematopoietic cells based on newborn NOD/SCID/beta2-microglobulin(null) mice. *Exp. Hematol.* 30: 488–494.
15. Mega, J., J. R. McGhee, and H. Kiyono. 1992. Cytokine- and Ig-producing T cells in mucosal effector tissues: analysis of IL-5- and IFN-gamma-producing T cells, T cell receptor expression, and IgA plasma cells from mouse salivary gland-associated tissues. *J. Immunol.* 148: 2030–2039.
16. Schulz, K. R., E. A. Danna, P. O. Krutzik, and G. P. Nolan. 2007. Single-cell phospho-protein analysis by flow cytometry. *Curr. Protoc. Immunol.* Chapter 8: Unit 8.17.
17. Niedergang, F., J. C. Sirard, C. T. Blanc, and J. P. Kraehenbuhl. 2000. Entry and survival of *Salmonella typhimurium* in dendritic cells and presentation of recombinant antigens do not require macrophage-specific virulence factors. *Proc. Natl. Acad. Sci. USA* 97: 14650–14655.
18. Baker, S. J., S. G. Rane, and E. P. Reddy. 2007. Hematopoietic cytokine receptor signaling. *Oncogene* 26: 6724–6737.
19. Semerad, C. L., F. Liu, A. D. Gregory, K. Stumpf, and D. C. Link. 2002. G-CSF is an essential regulator of neutrophil trafficking from the bone marrow to the blood. *Immunity* 17: 413–423.
20. Kawai, T., and S. Akira. 2010. The role of pattern-recognition receptors in innate immunity: update on Toll-like receptors. *Nat. Immunol.* 11: 373–384.
21. Opitz, B., V. van Laak, J. Eitel, and N. Suttorp. 2010. Innate immune recognition in infectious and noninfectious diseases of the lung. *Am. J. Respir. Crit. Care Med.* 181: 1294–1309.
22. Wissinger, E., J. Goulding, and T. Hussell. 2009. Immune homeostasis in the respiratory tract and its impact on heterologous infection. *Semin. Immunol.* 21: 147–155.
23. Savina, A., and S. Amigorena. 2007. Phagocytosis and antigen presentation in dendritic cells. *Immunol. Rev.* 219: 143–156.
24. Arinobu, Y., H. Iwasaki, M. F. Gurish, S. Mizuno, H. Shigematsu, H. Ozawa, D. G. Tenen, K. F. Austen, and K. Akashi. 2005. Developmental checkpoints of the basophil/mast cell lineages in adult murine hematopoiesis. *Proc. Natl. Acad. Sci. USA* 102: 18105–18110.
25. Hallgren, J., and M. F. Gurish. 2007. Pathways of murine mast cell development and trafficking: tracking the roots and routes of the mast cell. *Immunol. Rev.* 217: 8–18.
26. Kambe, N., H. Hiramatsu, M. Shimonaka, H. Fujino, R. Nishikomori, T. Heike, M. Ito, K. Kobayashi, Y. Ueyama, N. Matsuyoshi, et al. 2004. Development of both human connective tissue-type and mucosal-type mast cells in mice from hematopoietic stem cells with identical distribution pattern to human body. *Blood* 103: 860–867.
27. Manz, M. G. 2007. Human-hemato-lymphoid-system mice: opportunities and challenges. *Immunity* 26: 537–541.
28. Brooimans, R. A., J. Kraan, W. van Putten, J. J. Cornelissen, B. Löwenberg, and J. W. Gratama. 2009. Flow cytometric differential of leukocyte populations in normal bone marrow: influence of peripheral blood contamination. *Cytometry B Clin. Cytom.* 76B: 18–26.
29. Björnsson, S., S. Wahlström, E. Norström, I. Bernevi, U. O'Neill, E. Johansson, H. Runström, and P. Simonsson. 2008. Total nucleated cell differential for blood and bone marrow using a single tube in a five-color flow cytometer. *Cytometry B Clin. Cytom.* 74: 91–103.
30. Rathinam, C., W. T. Poueymirou, J. Rojas, A. J. Murphy, D. M. Valenzuela, G. D. Yancopoulos, A. Rongvaux, E. E. Eynon, M. G. Manz, and R. A. Flavell. 2011. Efficient differentiation and function of human macrophages in humanized CSF-1 mice. *Blood* 118: 3119–3128.
31. Rongvaux, A., T. Willinger, H. Takizawa, C. Rathinam, W. Auerbach, A. J. Murphy, D. M. Valenzuela, G. D. Yancopoulos, E. E. Eynon, S. Stevens, et al. 2011. Human thrombopoietin knockin mice efficiently support human hematopoiesis in vivo. *Proc. Natl. Acad. Sci. USA* 108: 2378–2383.
32. Willinger, T., A. Rongvaux, H. Takizawa, G. D. Yancopoulos, D. M. Valenzuela, A. J. Murphy, W. Auerbach, E. E. Eynon, S. Stevens, M. G. Manz, and R. A. Flavell. 2011. Human IL-3/GM-CSF knock-in mice support human alveolar macrophage development and human immune responses in the lung. *Proc. Natl. Acad. Sci. USA* 108: 2390–2395.
33. Takagi, S., Y. Saito, A. Hijikata, S. Tanaka, T. Watanabe, T. Hasegawa, S. Mochizuki, J. Kunisawa, H. Kiyono, H. Koseki, et al. 2012. Membrane-bound human SCF/KL promotes in vivo human hematopoietic engraftment and myeloid differentiation. *Blood* 119: 2768–2777.
34. Umeda, S., K. Takahashi, M. Naito, L. D. Shultz, and K. Takagi. 1996. Neonatal changes of osteoclasts in osteopetrosis (op/op) mice defective in production of functional macrophage colony-stimulating factor (M-CSF) protein and effects of M-CSF on osteoclast development and differentiation. *J. Submicrosc. Cytol. Pathol.* 28: 13–26.
35. Hu, X., and L. B. Ivashkiv. 2009. Cross-regulation of signaling pathways by interferon-gamma: implications for immune responses and autoimmune diseases. *Immunity* 31: 539–550.
36. McLemore, M. L., S. Grewal, F. Liu, A. Archambault, J. Poursine-Laurent, J. Haug, and D. C. Link. 2001. STAT-3 activation is required for normal G-CSF-dependent proliferation and granulocytic differentiation. *Immunity* 14: 193–204.
37. Kimura, A., M. A. Rieger, J. M. Simone, W. Chen, M. C. Wickre, B. M. Zhu, P. S. Hoppe, J. J. O'Shea, T. Schroeder, and L. Hennighausen. 2009. The transcription factors STAT5A/B regulate GM-CSF-mediated granulopoiesis. *Blood* 114: 4721–4728.
38. Elo, L. L., H. Järvenpää, S. Tuomela, S. Raghav, H. Ahlfors, K. Laurila, B. Gupta, R. J. Lund, J. Tahvanainen, R. D. Hawkins, et al. 2010. Genome-wide profiling of interleukin-4 and STAT6 transcription factor regulation of human Th2 cell programming. *Immunity* 32: 852–862.

39. Saraiva, M., J. R. Christensen, M. Veldhoen, T. L. Murphy, K. M. Murphy, and A. O'Garra. 2009. Interleukin-10 production by Th1 cells requires interleukin-12-induced STAT4 transcription factor and ERK MAP kinase activation by high antigen dose. *Immunity* 31: 209–219.
40. Graham, S. M., and M. English. 2009. Non-typhoidal salmonellae: a management challenge for children with community-acquired invasive disease in tropical African countries. *Lancet* 373: 267–269.
41. Liu, J., X. Guan, and X. Ma. 2007. Regulation of IL-27 p28 gene expression in macrophages through MyD88- and interferon-gamma-mediated pathways. *J. Exp. Med.* 204: 141–152.
42. MacNamara, K. C., K. Oduro, O. Martin, D. D. Jones, M. McLaughlin, K. Choi, D. L. Borjesson, and G. M. Winslow. 2011. Infection-induced myelopoiesis during intracellular bacterial infection is critically dependent upon IFN-γ signaling. *J. Immunol.* 186: 1032–1043.
43. Jambo, K. C., E. Sepako, R. S. Heyderman, and S. B. Gordon. 2010. Potential role for mucosally active vaccines against pneumococcal pneumonia. *Trends Microbiol.* 18: 81–89.
44. Legrand, N., A. Ploss, R. Balling, P. D. Becker, C. Borsotti, N. Brezillon, J. Debarry, Y. de Jong, H. Deng, J. P. Di Santo, et al. 2009. Humanized mice for modeling human infectious disease: challenges, progress, and outlook. *Cell Host Microbe* 6: 5–9.

ELSEVIER

Immune regulation and monitoring at the epithelial surface of the intestine

Jun Kunisawa[1,2] and Hiroshi Kiyono[1,2,3,4]

[1] Division of Mucosal Immunology, Department of Microbiology and Immunology, Institute of Medical Science, The University of Tokyo, Tokyo, Japan
[2] Department of Medical Genome Science, Graduate School of Frontier Science, The University of Tokyo, Tokyo, Japan
[3] Graduate School of Medicine, The University of Tokyo, Tokyo, Japan
[4] Core Research for Evolutional Science and Technology (CREST), Japan Science and Technology Agency, Tokyo, Japan

The intestinal enterocytes and other epithelial cells create physical barriers, including tight junctions and mucus layers. These cells also actively transport antibodies across the epithelium and simultaneously produce antimicrobial peptides and enzymes. These functions maintain intestinal homeostasis by allowing the selective absorption of nutrients and simultaneously preventing pathogenic infections. Recent evidence has revealed that both host-derived factors (e.g., cytokines) and gut environmental factors (e.g., commensal bacteria, dietary materials, and their metabolites) regulate the physical and immunological functions of the epithelium. Understanding the interactions between host cells and these environmental factors should help us to develop new strategies to prevent and treat immune diseases of the intestine.

The surface of the gastrointestinal tract is covered by a single layer of epithelium that separates the outside world from interstitial tissues. The intestinal epithelium is mainly composed of absorptive enterocytes (ECs) but also includes enteroendocrine, goblet, and Paneth cells [1]. Cross-communication among these cells enables the selective absorption of nutrients while simultaneously preventing the penetration of antigens and pathogens. The defense against pathogenic materials is at least partly achieved by the physical barriers of the epithelium, which include tight junctions and mucus layers. A large number of pathogens disrupt these barriers to access deeper tissues for dissemination [2,3]. The barriers also contribute to the establishment and maintenance of mucosal homeostasis. Indeed, a leaky intestinal barrier is one of the characteristics of chronic intestinal inflammatory diseases, such as inflammatory bowel disease and celiac disease [4,5].

Intestinal tissues also show intense immunological activity, and ECs contribute to the intestinal immune system by transporting and processing antibodies and associated antigens, by producing immunologically functional molecules, and by interacting with immunocompetent cells in the intestine [6]. Accumulating evidence has revealed that both host-derived factors (e.g. cytokines) and gut environmental factors (e.g. commensal bacteria, dietary materials, and their metabolites) engage in molecular crosstalk with the intestinal epithelium and affect intestinal barrier function and immune responses [7,8]. In this review, we focus on the immunological functions of ECs in the intestine and their regulation by commensal bacteria and dietary materials.

Physical barriers at the intestinal epithelium

Tight junctions

ECs provide a physical barrier to prevent the paracellular transport of luminal antigens and pathogens. Tight junctions are multifunctional complexes that are crucial for the maintenance of barrier integrity because they form a seal between adjacent ECs [9]. The tight junction regulates the absorption of nutrients, ions, and water while preventing the entry of pathogens into the host.

Tight junctions are composed of numerous interacting cellular proteins, including claudin, occludin, and zonula occludens (ZO) proteins (Fig. 1). Claudin and occludin are transmembrane proteins that seal the paracellular space between adjacent ECs. Among

Corresponding author:. Kunisawa, J. (kunisawa@ims.u-tokyo.ac.jp)

1359-6446/06/$ - see front matter http://dx.doi.org/10.1016/j.drudis.2012.08.001

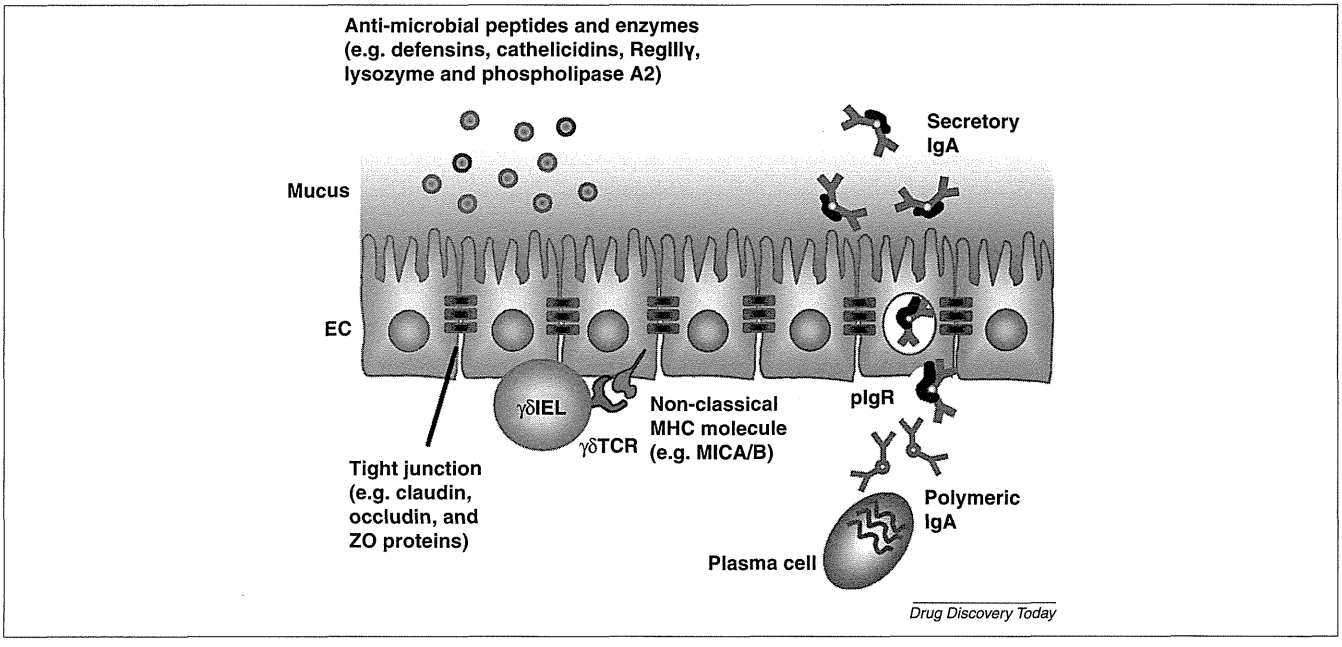

FIGURE 1

Physical and immunological barriers mediated by ECs. ECs (including Paneth cells) produce several molecules that create physical barriers in the intestine. They also produce antimicrobial peptides and enzymes, such as defensins, cathelicidins, RegIIIγ, lysozyme, and phospholipase A2 to kill the bacteria and establish a mucus layer to prevent bacterial attachment to the ECs. Tight junctions among ECs prevent bacterial penetration between the cells. ECs also have immunological functions. They express polymeric immunoglobulin receptor (pIgR), which binds and transports polymeric IgA produced from plasma cells into the intestinal lumen. ECs exposed to stresses (e.g. infection or cancer) express non-classical MHC molecules (e.g. MICA/B). MICA/B acts as a ligand for γδ T cell receptors, which are uniquely expressed on intraepithelial lymphocytes (γδIELs). *Abbreviations*: EC, enterocytes; MHC, major histocompatibility complex; ZO, zonula occludens.

the various types of claudins, claudin-1, -2, -3, -4, -5, -7, -8, -12, -15, -18, -20, and -23 are expressed in the intestinal epithelium [10,11]. ZO proteins are adaptors that connect transmembrane proteins; in particular, ZO-1 interacts with the claudin proteins and with F-actin in the intestinal ECs [12,13].

The physical barriers created by ECs are at least partly regulated by the immunological stimulation provided by commensal bacteria and dietary materials. Indeed, commensal and probiotic bacteria, their metabolites, food extracts, and dietary materials (e.g. fatty acids, polysaccharides, and flavonoids) have been shown to promote intestinal barrier integrity by increasing the expression of tight junction proteins [10].

Mucus

The mucus layer has been recognized as an important component in the intestine (Fig. 1). Mucin 2 (MUC2), a large glycoprotein characterized by variable O-linked glycans, is abundantly expressed by goblet cells located in the intestinal epithelium [14]. Generally, mucus can be divided into two layers. Although both layers have similar protein composition, the outer mucus layer is loose, whereas the inner mucus layer adheres firmly to the surface of the ECs. The firm mucus in the inner layer is an efficient barrier against pathogens [15]. In addition to the physical and biological barrier function of mucus, mucus also ensures the concentration of antimicrobial peptides and IgA antibodies at the surface of ECs. As similar to tight junctions, mucus expression is regulated by commensal bacteria, and the mucus layer of germ-free mice is thicker than that of specific pathogen-free mice [15].

Production of antimicrobial molecules at the epithelium

Antimicrobial peptides

The epithelium also secretes a variety of antimicrobial peptides [e.g. defensins, cathelicidins, and RegIIIγ (Fig. 1)]. The production of these peptides is mainly mediated by ECs and Paneth cells [16]. Paneth cells reside at the base of the crypt regions of the intestine, where they constitutively produce α-defensins. This does not require bacterial stimulation, because Paneth cells produce normal amounts of α-defensin in germ-free mice [17]. By contrast, ECs require microbial stimulation for the production of β-defensins [16]. ECs also produce cathelicidin, the expression of which is regulated by short-chain fatty acids produced when polysaccharides are metabolized by fermenting bacteria [18]. Both defensins and cathelicidin are cationic small peptides that exhibit antimicrobial activity by damaging and permeabilizing the bacterial cell membrane by pore formation [19].

RegIIIγ is a C-type lectin produced by ECs and Paneth cells in the ileum, where it kills Gram-positive bacteria by binding to surface-exposed carbohydrate moieties of peptidoglycans [20]. Commensal bacteria, especially Gram-negative bacteria, induce RegIIIγ expression on ECs, and a recent study demonstrated that MyD88 intrinsically expressed on ECs controls the production of RegIIIγ, which establishes the physical separation between the microbiota and the intestinal epithelial surface [21].

Unlike RegIIIγ, which specifically targets Gram-positive bacteria, bactericidal and/or permeability-increasing protein (BPI) shows antimicrobial activity against Gram-negative bacteria. The high affinity of BPI for lipopolysaccharide (LPS) leads to the

destabilization of the outer membrane of Gram-negative bacteria and also neutralizes LPS-induced inflammation [22].

Antimicrobial enzymes

Antimicrobial activity is also mediated by bacteriolysis enzymes (e.g. secretory phospholipase A2 and lysozyme). Phospholipase A2 is a small enzyme produced by Paneth cells that degrades bacterial phospholipids and subsequently disrupts the integrity of Gram-positive and -negative bacteria [23]. Phospholipase A2 enzyme activity is normal in the intestine of germ-free rats [24], but caloric restriction increases the gene expression of lysozyme and phospholipase A2 [25]. Therefore, it is likely that nutritional conditions rather than commensal bacteria regulate the activity of these antimicrobial enzymes in the intestine. Lysozyme is produced by Paneth cells and ECs. Its bactericidal activity derives from its cleavage of the glycosidic linkage between *N*-acetylglucosamine and *N*-acetyl muramic acid of peptidoglycan. Because Gram-positive bacteria express more peptidoglycan than Gram-negative bacteria, lysozyme acts preferentially on Gram-positive bacteria.

Transport of antibodies through ECs

IgA transport mediated by polymeric immunoglobulin receptors

One function of the epithelial immune barrier is to transport antibodies across the barrier. ECs express polymeric immunoglobulin receptors (pIgR) for the transport of polymeric forms of IgA (pIgA) and IgM (pIgM) in the basal-to-apical direction in association with an extracellular proteolytic fragment of the pIgR (known as the secretory component) [26]; together, the IgA and the secretory component form secretory immunoglobulin A (S-IgA). After S-IgA is secreted into the intestinal lumen, it inhibits adherence of pathogens to host ECs in the intestine and neutralizes pathogenic toxins by binding to their biologically active sites (Fig. 1) [27]. Additionally, IgA is able to exclude antigens and pathogens from the intestinal secretions while it is transported through ECs, and it also prevents viral replication inside ECs [28,29].

In addition to the function of S-IgA in the immunosurveillance, several lines of evidence demonstrate that S-IgA has a key role in preventing the penetration and/or growth of commensal bacteria [30]. These functions of S-IgA achieve the immune responses against commensal bacteria restricted in the intestinal but not systemic immune compartments in normal mice, while IgA-deficient mice exhibited systemic IgG responses against commensal bacteria [31–33]. A recent study also demonstrated that, in the absence of IgA, commensal bacteria-derived stimulation induced the increased expression of interferon-regulated genes in the ECs for the compensatory immunosurveillance with simultaneous reduction of lipid metabolism-related Gata4-regulated genes, which resulted in the lipid malabsorption and decreased lipid deposition [34]. Thus, S-IgA mediates the regulation between ECs and commensal bacteria, which is important not only for the maintenance of immunological homeostasis but also for metabolism [34].

Neonatal Fc receptor for IgG transport

Another receptor for immunoglobulin is the neonatal Fc receptor for IgG (FcRn). Although early studies in rodents indicated that FcRn was responsible for the passive acquisition of IgG neonatally, subsequent studies indicated that FcRn is also expressed by adult human epithelium and antigen-presenting cells in the intestine and thus is not strictly limited to neonatal life [35]. Unlike pIgR mentioned above, human FcRn binds IgG and the transport pathway is bidirectional, both apical to basal and basal to apical [36]. The bidirectional transport of IgG enables retrieval of intestinal antigens in a complex with IgG into the intestinal lamina propria, where the antigen and/or IgG complexes are subsequently taken up by antigen-presenting cells to prime T cell responses [37].

Intraepithelial T lymphocytes

The epithelium also includes lymphocytes that are commonly termed intraepithelial lymphocytes (IELs) [38]. IELs reside between the basolateral surfaces of ECs, and one IEL occurs for every 4–10 ECs in the small intestine and for every 30–50 ECs in the large intestine.

Most IELs are T cells. As similar to T cells observed at other sites (e.g. spleen and intestinal lamina propria), some portions of IELs express αβ T cell receptors and act as cytotoxic T lymphocytes by recognizing antigenic peptides presented by classical major histocompatibility complex (MHC) molecules on pathogenic ECs (e.g. microbe-infected cells) and killing them by producing cytotoxic molecules (e.g. perforin and granzymes) [38]. Other IELs express the γδ T cell receptor (and are therefore known as γδIELs) and show minimal pathogen-specific activity [38,39]. The innate immune function of γδIELs enables the rapid removal of infected ECs. To recognize the infected ECs, non-classical MHC molecules, such as MHC class I chain-related protein A/B (MICA/B) in human, act as ligands for γδIELs. MICA/B is generally not expressed on ECs, but is induced by stresses such as heat shock and microbial infections. The activated γδIELs then synthesize an array of cytokines, including interleukin (IL)-2, IL-3, IL-6, interferon (IFN)-γ, tumor necrosis factor (TNF)-α, and transforming growth factor (TGF)-β, and cytotoxic molecules, such as perforin, granzyme, and Fas ligand to kill the microbe-infected ECs [38].

Epithelium senses signals from commensal bacterial in the regulation of T cell differentiation in the intestine

The immune system requires interactions with commensal bacteria for its development. Toll-like receptors (TLRs) act as sensors of commensal bacteria although they were initially discovered as pathogen recognition receptors. ECs express several kinds of TLRs and the ligands from commensal bacteria promote immunological functions of Ecs, such as IgA transport, tight junctions, and expression of antimicrobial peptides [40]. Of note, ECs have unique expression profiles and spatially restricted distribution (apical vs. basolateral) of TLRs together with unique underlying signaling pathways, which enables the prevention of deleterious inflammatory responses in the intestine [40].

Because commensal bacteria express shared molecules which act as a ligand of TLRs, it was previously thought that unspecified commensal bacteria indiscriminately induced the development of the immune system; however, accumulating evidence has demonstrated that individual species of commensal bacteria have specific roles in the determination of immunological balance by regulating T cell differentiation in the intestine [8]. ECs have an important role in this pathway.

Segmented filamentous bacteria induce the differentiation of Th17 cells

Several groups have shown that segmented filamentous bacteria (SFB) induce components of the active immune system, including IgA-producing cells, γδIELs, and IL-17-producing T (Th17) cells [41–43]. SFB colonization on ECs results in the production of serum amyloid A, which acts on intestinal dendritic cells (DCs) to enhance the production of IL-6 and IL-23 [43]. Because these two cytokines are Th17 cell-inducing cytokines, the immunological environment mediated by SFB, ECs, and DCs results in the preferential induction of Th17 cells in the intestine.

Preferential induction of Treg cells in the colon by Clostridium *clusters IV and XIVa*

Another form of crosstalk between ECs and commensal bacteria in the regulation of T cell differentiation is mediated by *Clostridium* clusters IV and XIVa (also known as the *Clostridium leptum* and *coccoides* groups) [44]. By contrast to the effects of SFB, colonization by *Clostridium* clusters IV and XIVa induces regulatory T (Treg) cells in the colon to achieve quiescent immunity. *Clostridium* clusters IV and XIVa form a thin colonizing layer on the epithelium, where they enhance the release of the active form of TGF-β by increasing the expression of matrix metalloproteinases that convert latent TGF-β into the active form. Because TGF-β is an essential cytokine for the differentiation of Treg cells from naive T cells, colonization with these *Clostridium* species converts non-Treg cells into Treg cells locally in the colon with little effect on thymus-derived Treg cells.

Dietary metabolites regulate intestinal immunity through the epithelium

Nutritional materials also influence intestinal immunity, and commensal bacteria are involved in metabolizing indigestible dietary materials into biologically active metabolites. Dietary materials (e.g. polysaccharides, vitamins, and lipids) and their metabolites contribute to the regulation of intestinal immunity (Fig. 2).

Polysaccharides

Dietary polysaccharides and endogenous mucus in the intestine are digested and metabolized into short-chain fatty acids, such as acetate, butyrate, and propanoate, by bacterial fermentation. These short-chain fatty acids are an energy source for ECs and affect immune cell functions. For example, acetate and butyrate maintain epithelial barrier function by stimulating the release of mucin and by facilitating the maintenance of epithelial integrity [45,46]. Acetate and butyrate also regulate the proliferation of ECs and their production of cytokines [47,48]. In addition, acetate modulates the immunological function of neutrophils that express G-protein-coupled receptor 43 [GPR43, also known as free fatty acid receptor 2 (FFAR2)], a receptor for the short-chain fatty acids. Neutrophils lacking GPR43 show decreased levels of phagocytic activity and lower production of reactive oxygen species, but also are more responsive to chemoattractants such as C5a and inflammatory chemokines [49]. Consistent with these findings, intestinal inflammation is exacerbated in GPR43-deficient mice.

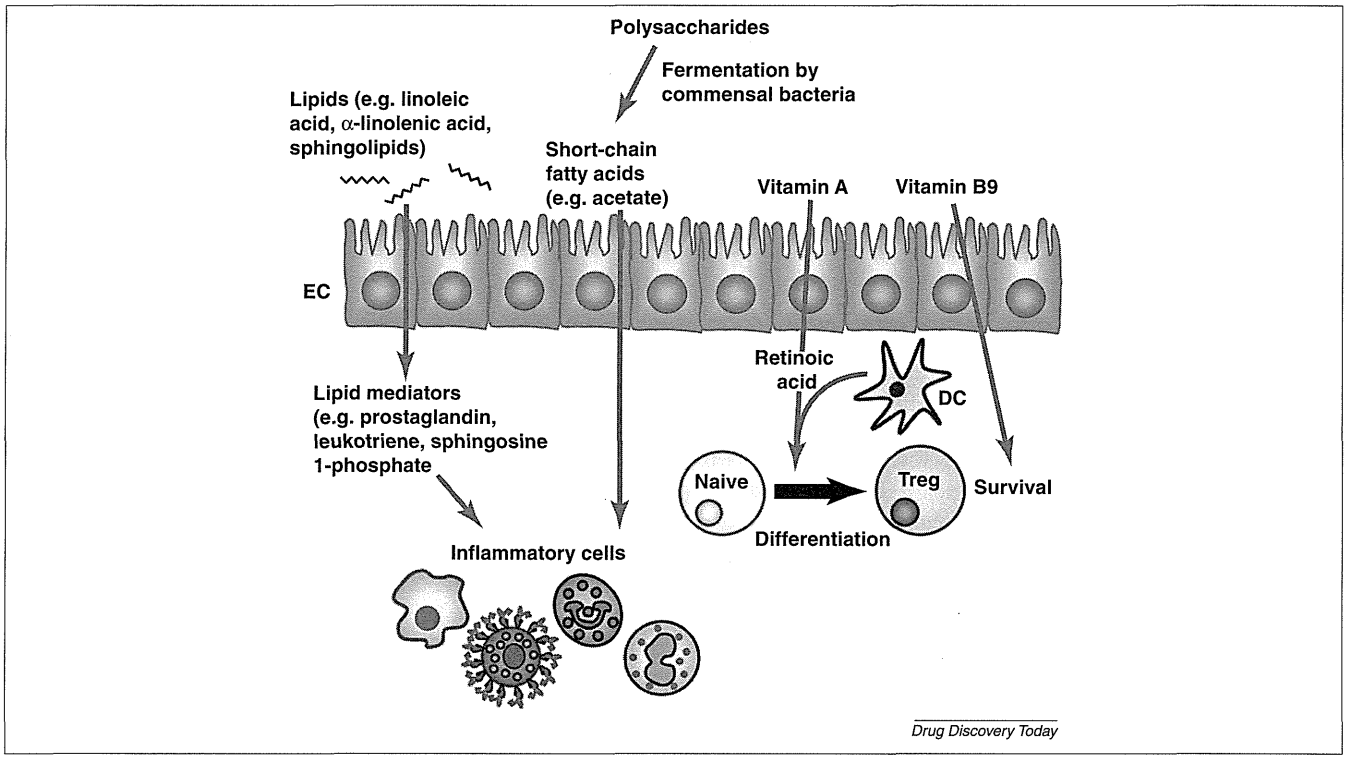

FIGURE 2

Dietary materials in the regulation of EC functions. Dietary lipids are metabolized into lipid mediators, and short-chain fatty acids are generated by fermentation of polysaccharides by commensal bacteria. These products positively or negatively regulate the functions of inflammatory cells. ECs also absorb vitamin A, and both ECs and dendritic cells (DCs) metabolize vitamin A into retinoic acid, which preferentially induces regulatory T (Treg) cells from naive T cells. The differentiated Treg cells require vitamin B9 for their survival. *Abbreviation:* EC, enterocytes.